Supporting Information

for

Combining gold(I/III) complexes and ferrociphenol scaffolds for the generation of bimetallic complexes with anticancer activity

Magda Křelinová,[a] Jérémy Forté,[b] Tom Lacoma,[b] Giulia Annesi,[c] Alessandra Folda,[c] Maria Pia Rigobello,[c] Michèle Salmain,[b] Petr Štěpnička,[a] Jiří Schulz[a] and Benoît Bertrand[b]**

[a] Department of Inorganic Chemistry, Faculty of Science, Charles University, Hlavova 2030, 128 00 Prague, Czech Republic, E-mail: jiri.schulz@natur.cuni.cz

[b] Sorbonne Université, CNRS, Institut Parisien de Chimie Moléculaire, 4 place Jussieu, 75005 Paris, France; E-mail : benoit.bertrand@sorbonne-universite.fr

[c] Department of Biomedical Sciences, University of Padua, Via Ugo Bassi 58/b, 35121 Padova, Italy

s

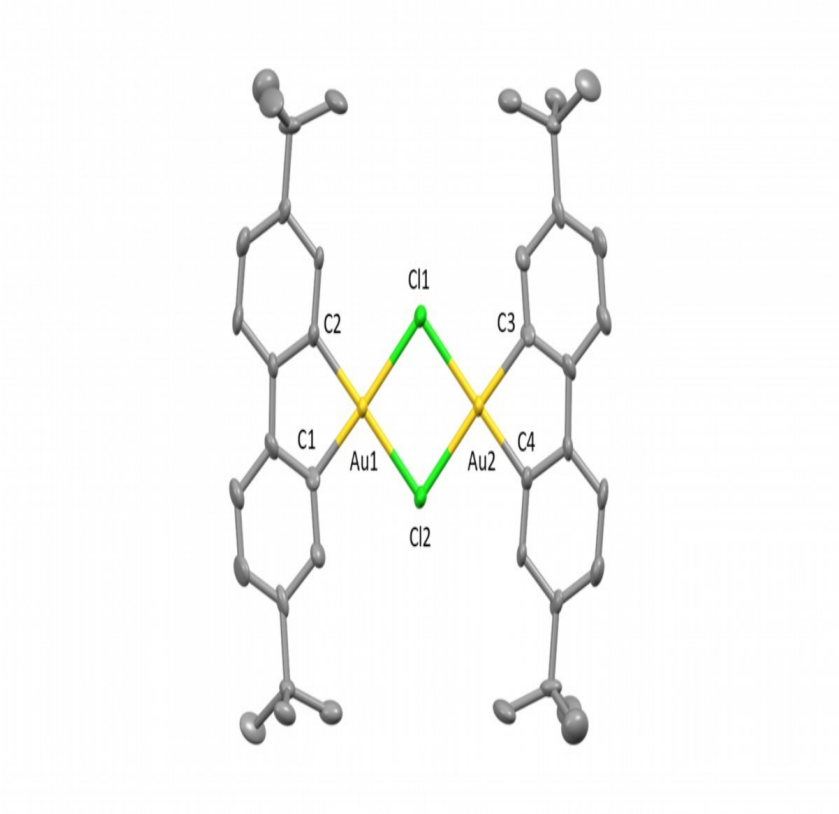

Figure S1: Crystal structure of the dimeric precursor **[(C^C)AuCl]$_2$**. Ellipsoids set at 50% probability. Hydrogen atoms have been omitted for clarity. Selected bond distances [Å] and angles [°] measured at 200 K: Au1-C1 2.000(16), Au1-C2 1.993(15), Au1-Cl1 2.432(4), Au1-Cl2 2.421(5), Au2-C4 2.000(16), Au2-C3 1.993(15), Au2-Cl1 2.421(5), Au2-Cl2 2.432(4), Cl2-Au1-C1 98.5(4), C1-Au1-C2 80.8(5), C2-Au1-Cl2 96.9(4), Cl1-Au1-Cl2 83.91(16), Cl2-Au2-C4 98.5(4), C4-Au2-C3 80.8(5), C3-Au1-Cl1 96.9(4), Cl1-Au1-Cl2 83.91(16).

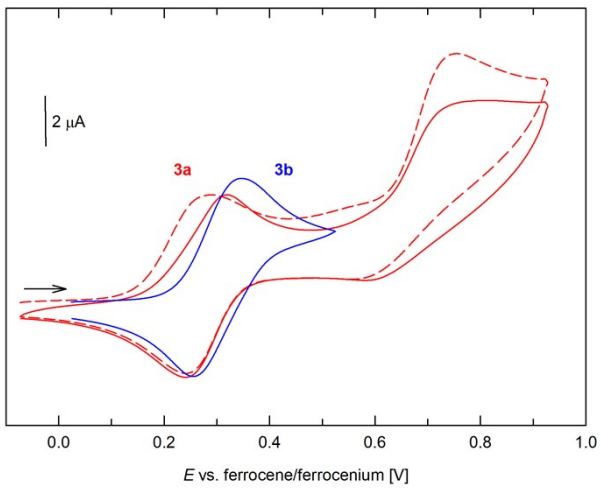

Figure S2. Cyclic voltammograms of **3a** and **3b** recorded at a Pt disc electrode in 0.1 M $Bu_4N[PF_6]/CH_2Cl_2$ and at 100 mV s^{-1} scan rate (for **3a**, the second scan is shown by a dashed line).

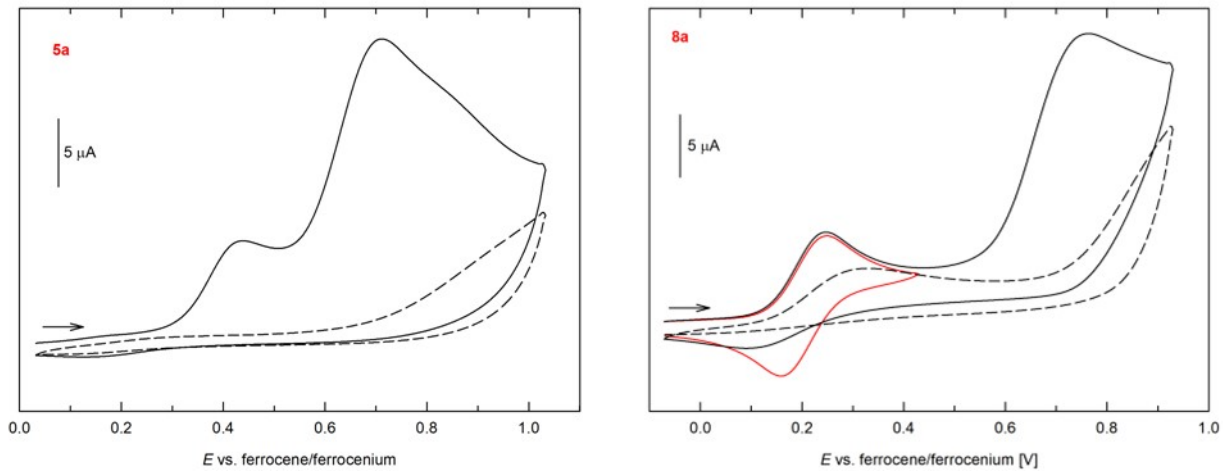

Figure S3. Cyclic voltammograms of **5a** (left) and **8a** (right) recorded at a Pt disc electrode in 0.1 M $Bu_4N[PF_6]/CH_2Cl_2$ and at 100 mV s^{-1} scan rate (the second scans are shown by dashed lines).

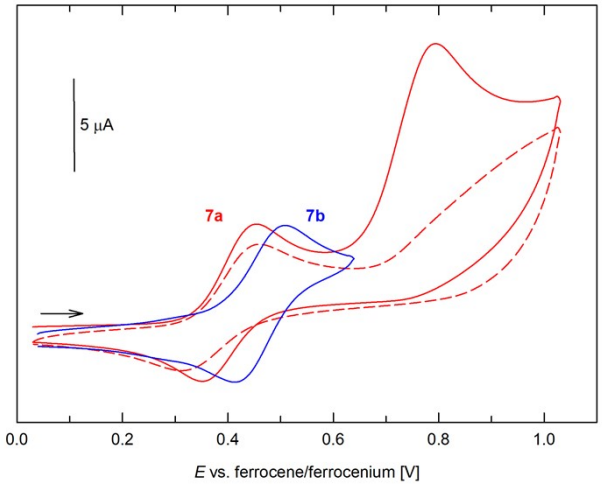

Figure S4. Cyclic voltammograms of **7a** and **7b** recorded at a Pt disc electrode in 0.1 M $Bu_4N[PF_6]/CH_2Cl_2$ and at 100 mV s^{-1} scan rate (for **7a**, the second scan is shown by a dashed line).

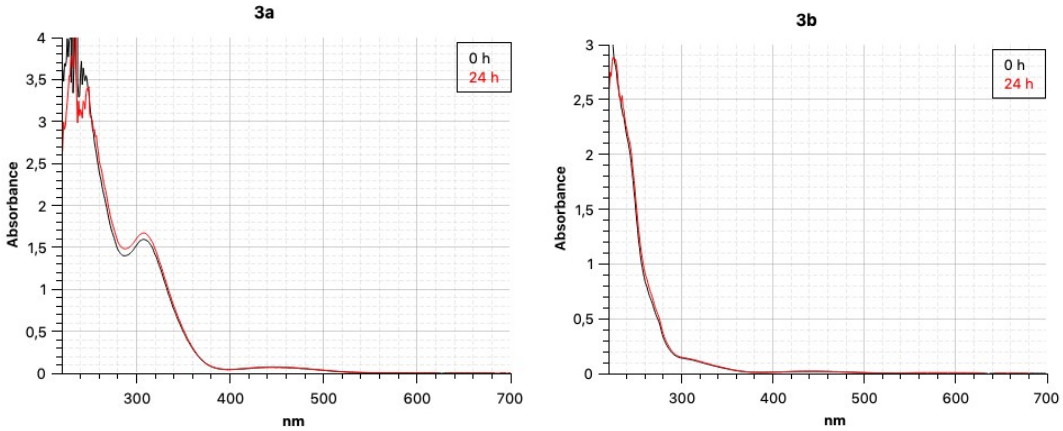
3a
0 h
24 h
Absorbance
nm

3b
0 h
24 h
Absorbance
nm

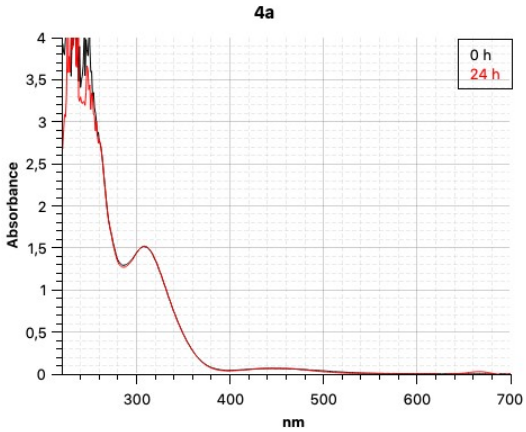
4a
0 h
24 h
Absorbance
nm

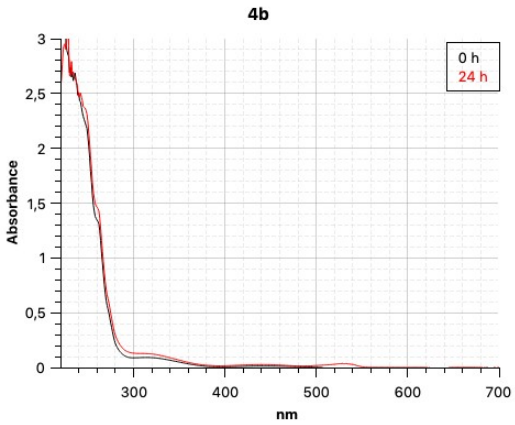
4b
0 h
24 h
Absorbance
nm

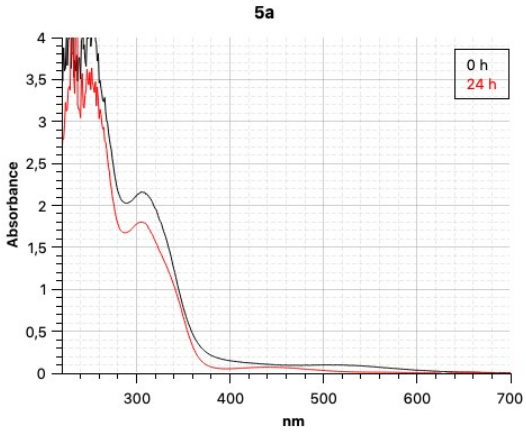
5a
0 h
24 h
Absorbance
nm

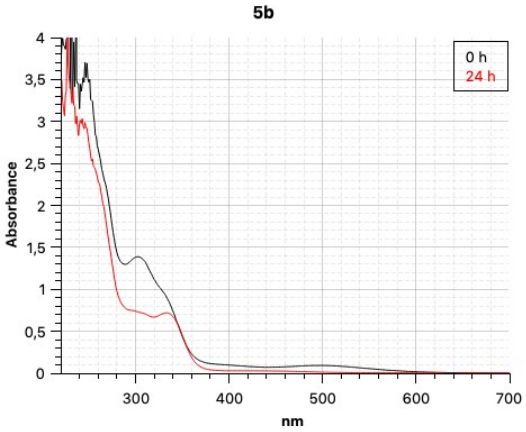
5b
0 h
24 h
Absorbance
nm

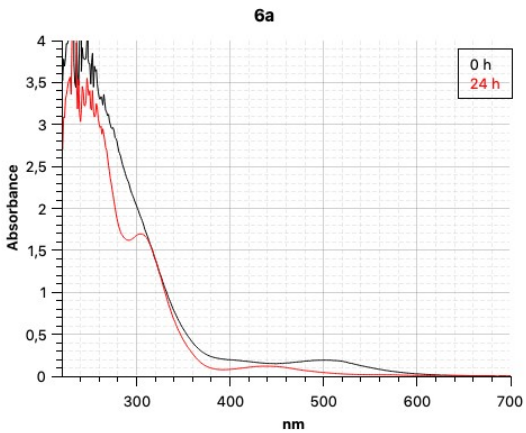
6a
0 h
24 h
Absorbance
nm

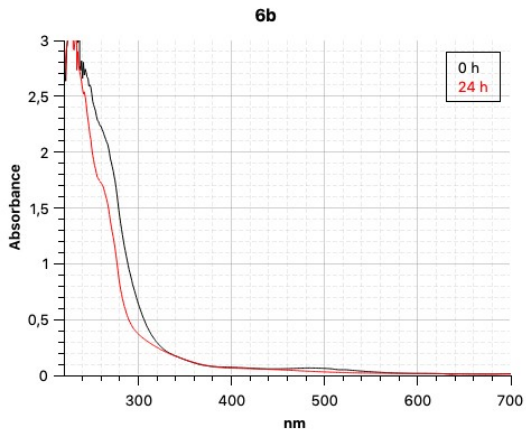
6b
0 h
24 h
Absorbance
nm

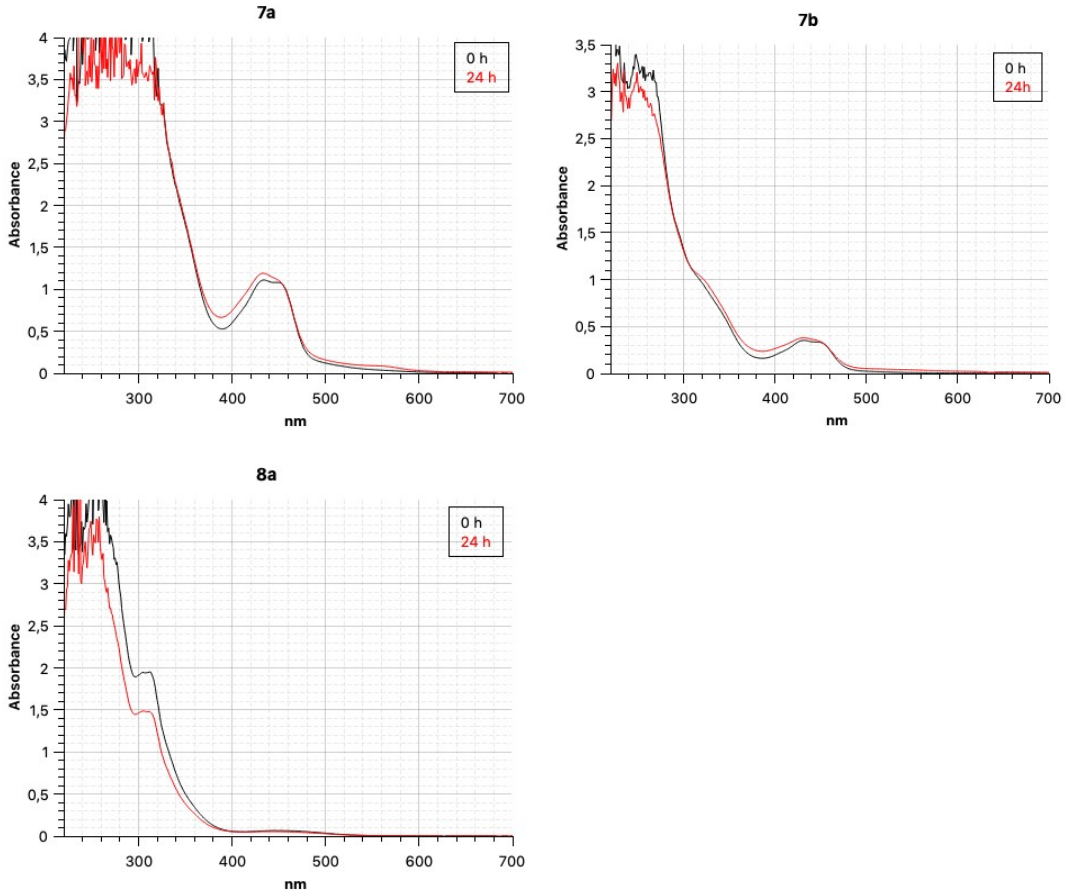

Figure S5: Stability studies of complexes **3a/b**, **4a/b**, **5a**, **6a/b**, **7a/b** and **8a** (100 µM) in a mixture 50/50 MeCN/PBS after different incubation times at 37 °C.

Table S1. Characterization of complexes (100 µM in PBS/MeCN 1:1) by UV-visible spectroscopy

compound	λ_{max} (nm) ; Abs	
	0 h	24 h, 37°C
3a	307 ; 1.595 ; 451 ; 0.07	307 ; 1.67 ; 451 ; 0.074
3b	444 ; 0.019	441 ; 0.021
4a	307 ; 1.517 ; 448 ; 0.068	307 ; 1.517 ; 448 ; 0.068
4b	313 ; 0.09 ; 441 ; 0.013	309 ; 0.127 ; 440 ; 0.026
5a	305 ; 2.15 ; 505 ; 0.1	305 ; 1.804 ; 440 ; 0.073
5b	302 ; 1.388 ; 491 ; 0.092	333 ; 0.72
6a	502 ; 0.192	305 ; 1.7 ; 440 ; 0.119
6b	484 ; 0.066	no bands observed
7a	434 ; 1.11	434 ; 1.19
7b	432 ; 0.352	432 ; 0.379
8a	310 ; 1.95 ; 305 ; 1.95 ; 447 ; 0.066	310 ; 1.48 ; 305 ; 1.49 ; 443 ; 0.054

Table S2: EC_{50} after 72 h incubation of complexes **1a**, **2-4a/b**, **5a**, **6-7a/b**, ferrociphenol and cisplatin against MDA-MB-231, A549 and MCF-10A cells.

Compound	EC_{50} (μM)			Selectivity index-1[c]	Selectivity index-2[c]
	MDA-MB-231	A549	MCF-10A		
1a[a]	6.4 ± 1.1	8.2 ± 0.9	10.6 ± 1.0	1.65	1.3
2a	5.3 ± 0.8	11.3 ± 1.8	3.5 ± 1.0	0.66	0.31
2b	1.4 ± 0.4	3.4 ± 0.1	0.22 ± 0.02	0.16	0.06
3a	1.1 ± 0.1	2.7 ± 0.7	1.0 ± 0.5	0.9	0.37
3b	0.31 ± 0.05	1.6 ± 0.1	0.19 ± 0.01	0.61	0.12
4a	1.47 ± 0.07	3.4 ± 0.5	1.4 ± 0.3	0.95	0.41
4b	0.23 ± 0.02	0.46 ± 0.06	0.21 ± 0.01	0.91	0.46
5a	1.80 ± 0.07	3.9 ± 0.3	1.1 ± 0.2	0.61	0.28
6a	5.6 ± 0.2	13.0 ± 0.3	1.1 ± 0.5	0.2	0.08
6b	1.8 ± 0.1	16.0 ± 3.0	0.9 ± 0.4	0.5	0.06
7a	1.7 ± 0.2	5.5 ± 0.2	0.8 ± 0.3	0.47	0.15
7b	1.91 ± 0.01	4.7 ± 0.2	1.0 ± 0.3	0.53	0.21
Ferrociphenol[a]	2.5 ± 0.2	0.9 ± 0.2	3.0 ± 0.2	1.2	3.3
cisplatin[b]	20.4 ± 3.4	1.7 ± 0.5 μM	3.2 ± 0.8	0.16	1.9

[a] See reference 1. [b] See reference 2. [c] selectivity index-1 = EC_{50}(MCF10-A) / EC_{50}(MDA-MB-231); selectivity index-2 = EC_{50}(MCF10-A) / EC_{50}(A549)

Table S3. EC_{50} ratios of pairs of compounds

compounds pairs	EC_{50} ratio	
	MDA-MB-231	A549
2b/2a	0.26	0.3
3b/3a	0.28	0.59
4b/4a	0.34	0.24
6b/6a	0.32	1.23
7b/7a	1.12	0.85

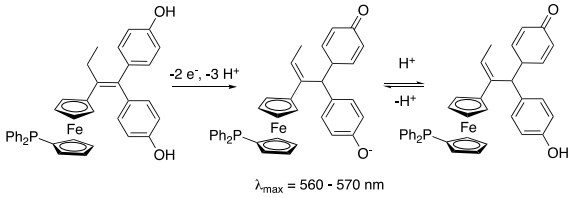

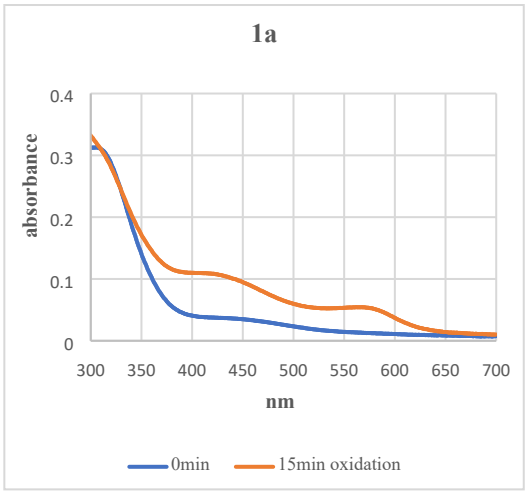

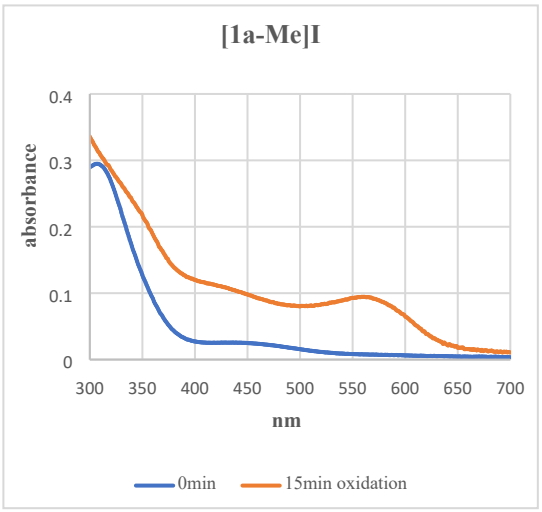

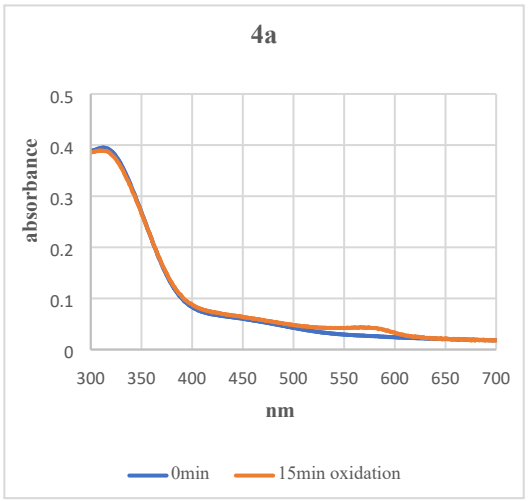

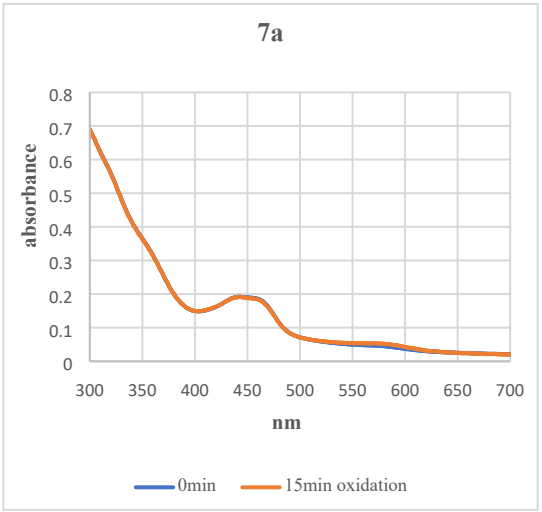

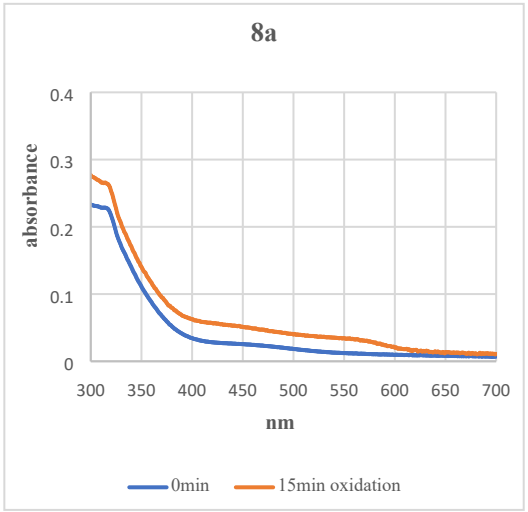

Figure S6. Time evolution of the UV/Vis spectra of **1a**, **[1a-Me]I**, **4a**, 7a and **8a** (25 µM) in the presence of HRP (22 nM) and H_2O_2 (100 µM) at pH 7.4 (0.2 M Na-K-Pi buffer, 5 mM EDTA, 0.5% DMSO). Formation of the quinone methide in the phenolate form (scheme for compound **1a** in the upper left panel) is assessed by the presence of a band at ca. 560 nm on the spectra recorded after 15 min reaction.

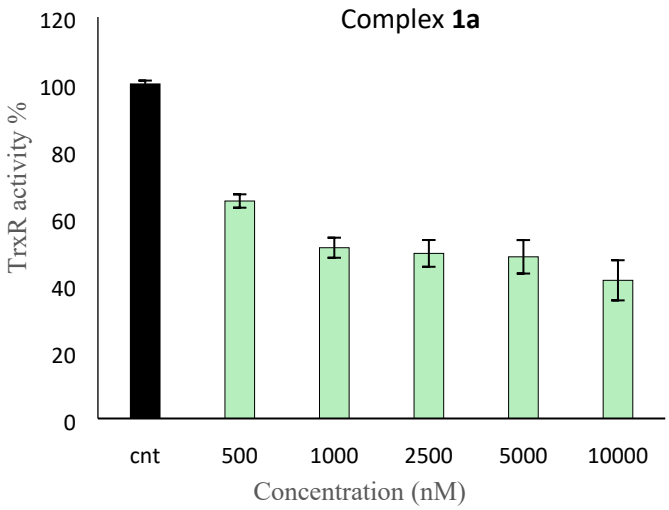
Complex 1a
TrxR activity %
120
100
80
60
40
20
0
cnt
500
1000
2500
5000
10000
Concentration (nM)

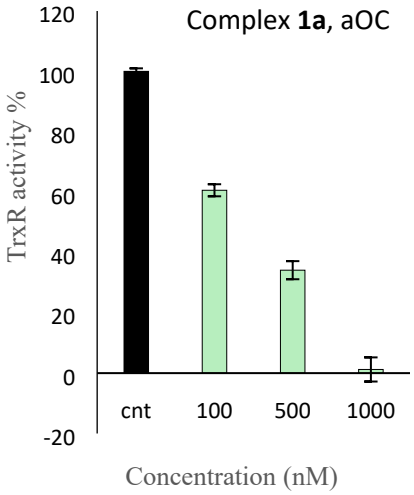
Complex 1a, aOC
TrxR activity %
120
100
80
60
40
20
0
-20
cnt
100
500
1000
Concentration (nM)

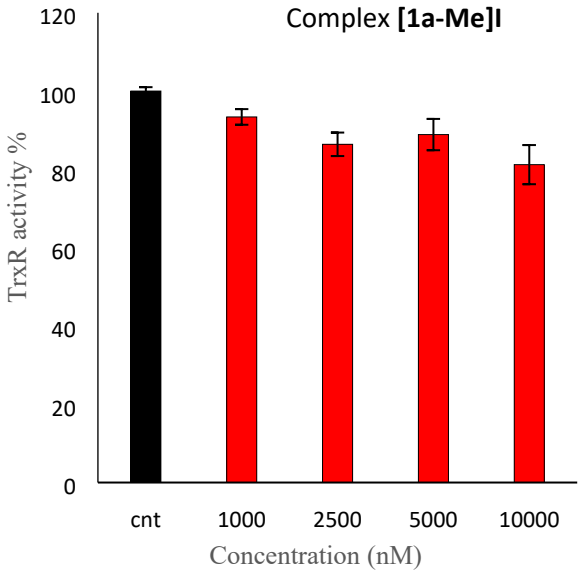
Complex [1a-Me]I
TrxR activity %
120
100
80
60
40
20
0
cnt
1000
2500
5000
10000
Concentration (nM)

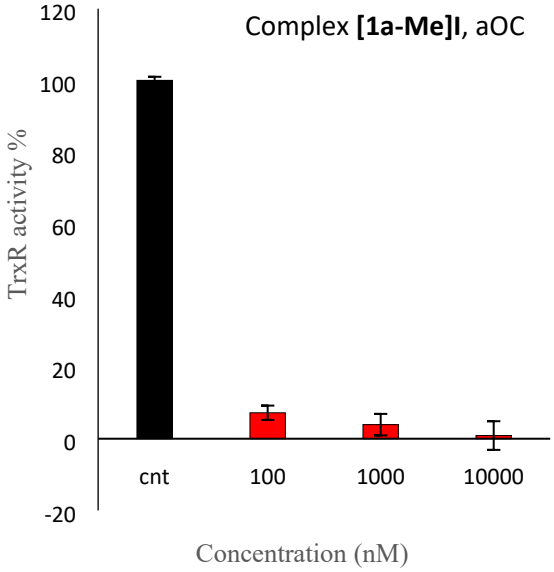
Complex [1a-Me]I, aOC
TrxR activity %
120
100
80
60
40
20
0
-20
cnt
100
1000
10000
Concentration (nM)

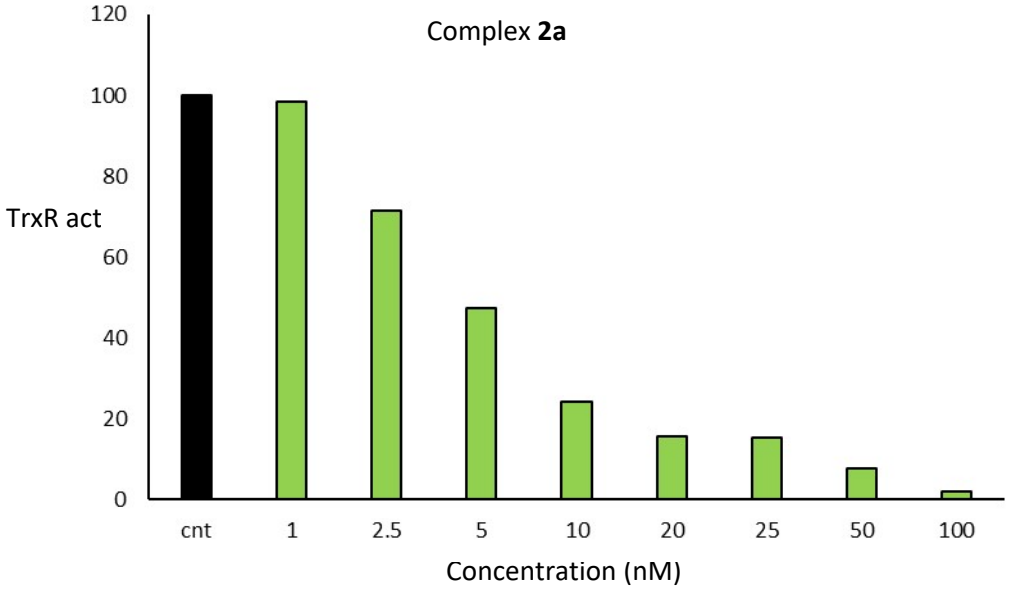
Complex 2a
TrxR act
120
100
80
60
40
20
0
cnt
1
2.5
5
10
20
25
50
100
Concentration (nM)

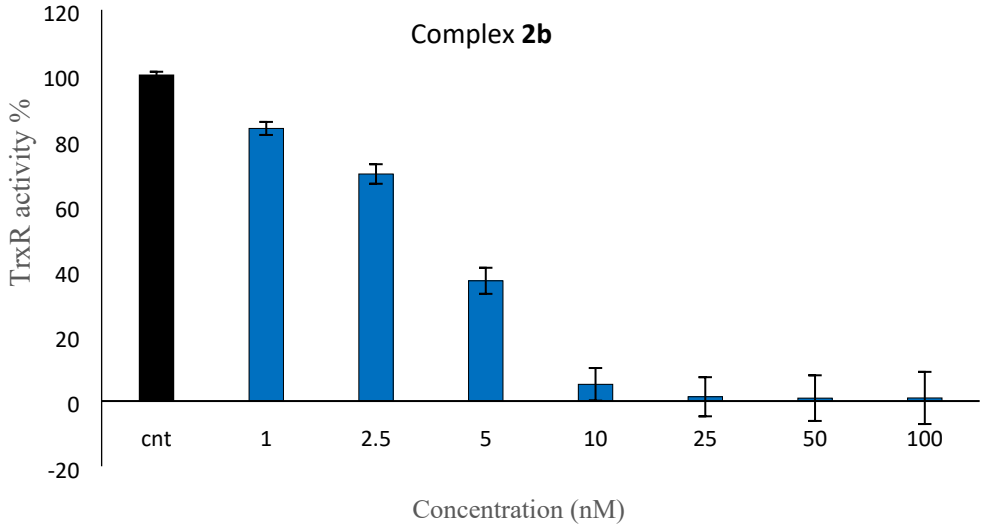
Complex 2b
TrxR activity %
120
100
80
60
40
20
0
-20
cnt
1
2.5
5
10
25
50
100
Concentration (nM)

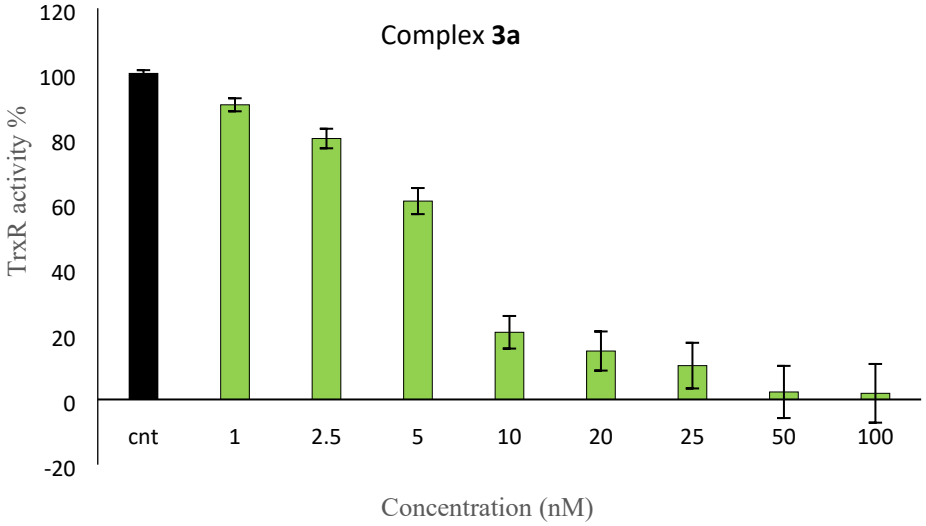
Complex 3a
TrxR activity %
120
100
80
60
40
20
0
-20
cnt
1
2.5
5
10
20
25
50
100
Concentration (nM)

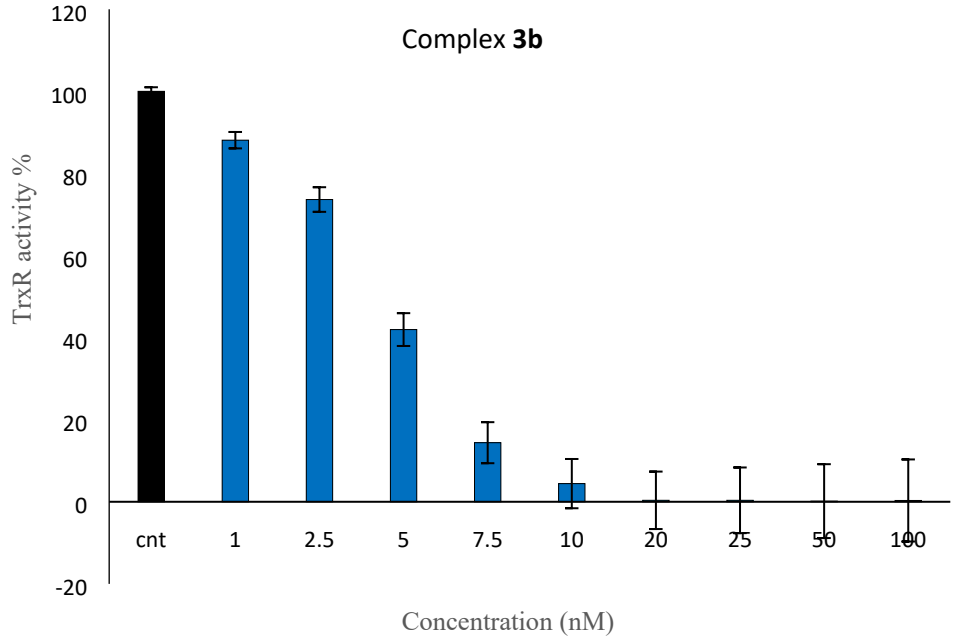
Complex 3b
TrxR activity %
120
100
80
60
40
20
0
-20
cnt
1
2.5
5
7.5
10
20
25
50
100
Concentration (nM)

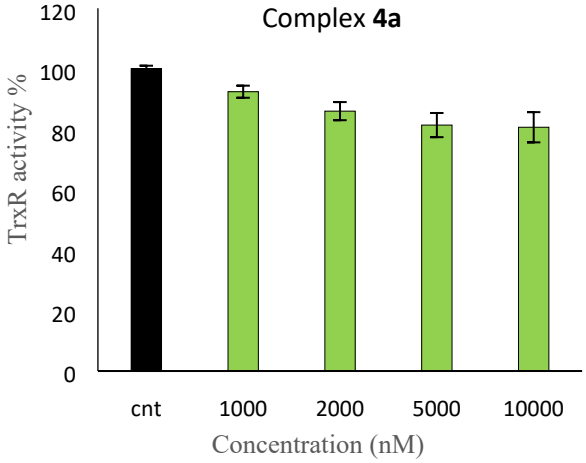
Complex 4a
TrxR activity %
120
100
80
60
40
20
0
cnt
1000
2000
5000
10000
Concentration (nM)

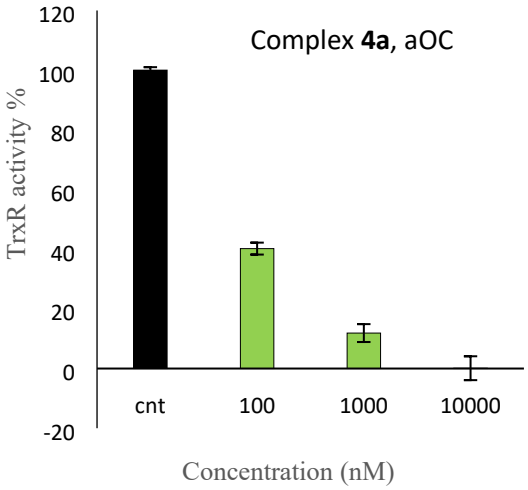
Complex 4a, aOC
TrxR activity %
120
100
80
60
40
20
0
-20
cnt
100
1000
10000
Concentration (nM)

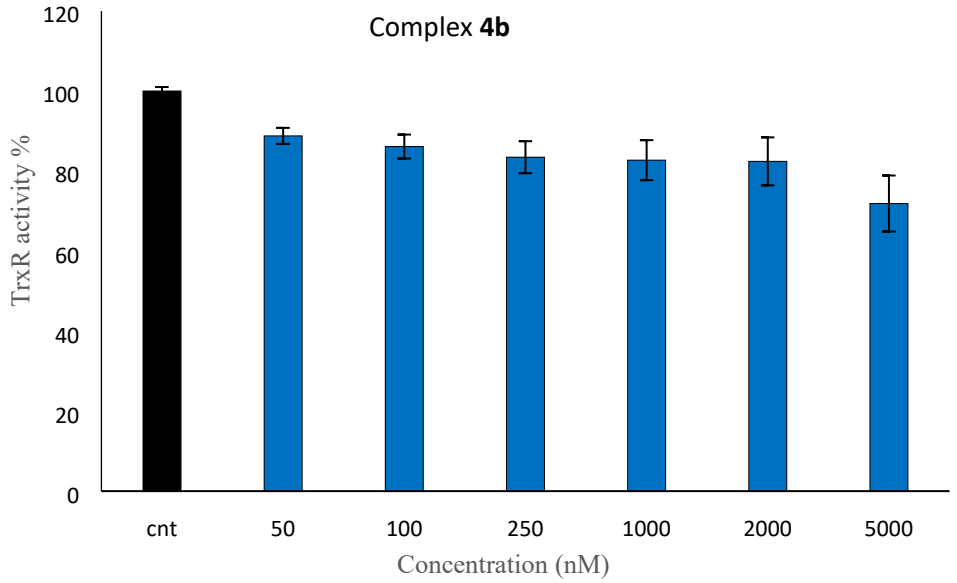
Complex 4b
TrxR activity %
120
100
80
60
40
20
0
cnt
50
100
250
1000
2000
5000
Concentration (nM)

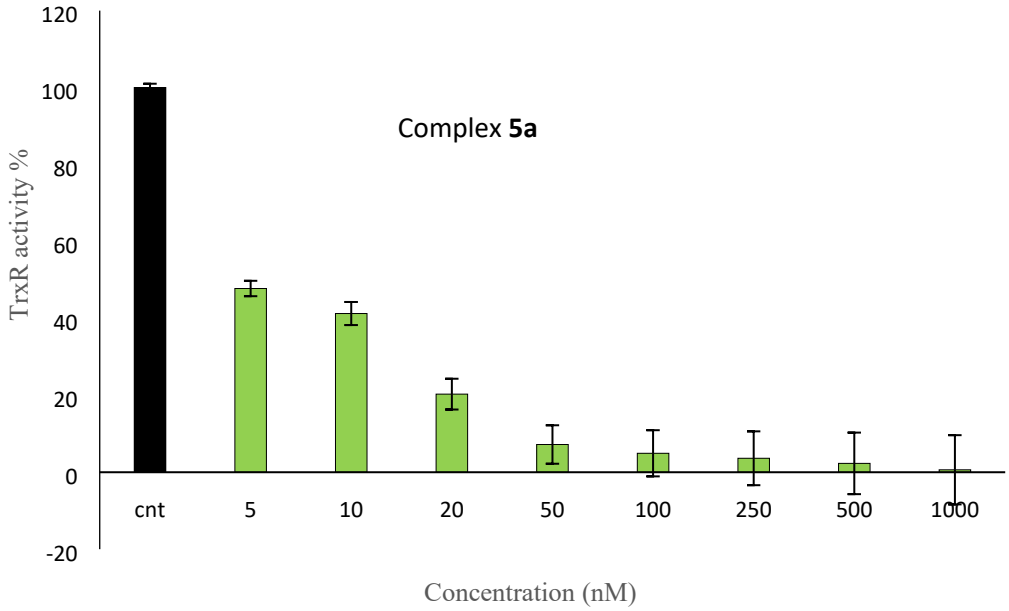
Complex 5a
TrxR activity %
120
100
80
60
40
20
0
-20
cnt
5
10
20
50
100
250
500
1000
Concentration (nM)

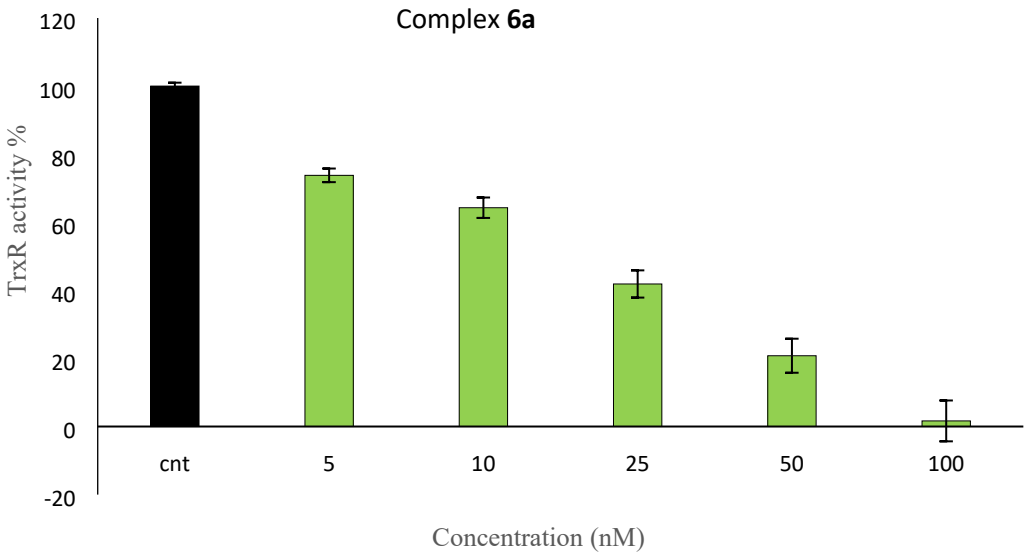
Complex 6a
TrxR activity %
120
100
80
60
40
20
0
-20
cnt
5
10
25
50
100
Concentration (nM)

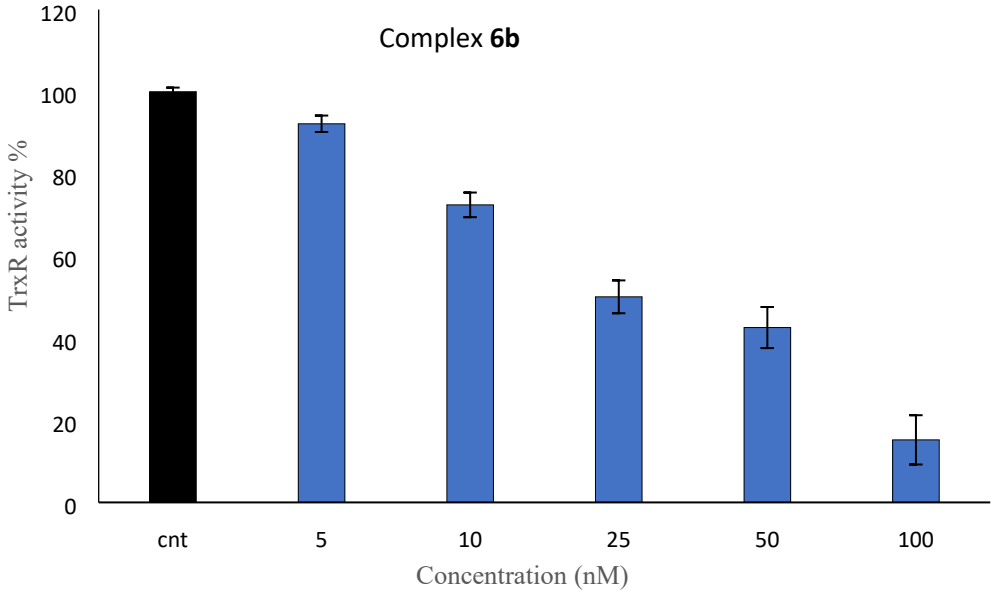
Complex 6b
TrxR activity %
120
100
80
60
40
20
0
cnt
5
10
25
50
100
Concentration (nM)

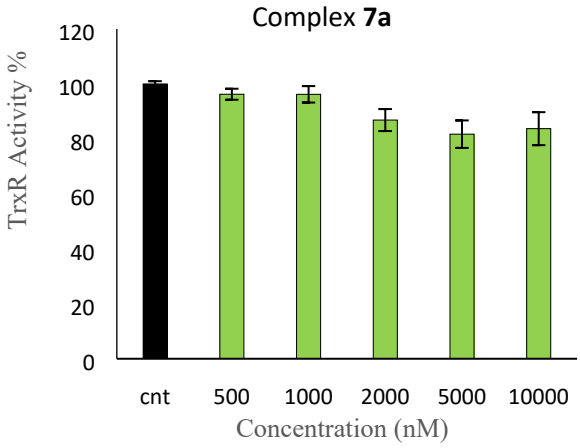
Complex 7a
TrxR Activity %
120
100
80
60
40
20
0
cnt
500
1000
2000
5000
10000
Concentration (nM)

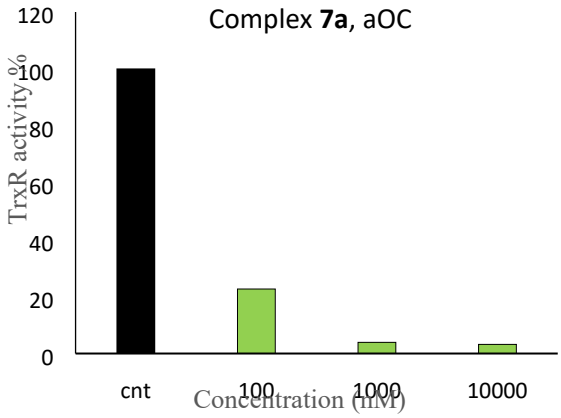
Complex 7a, aOC
TrxR activity %
120
100
80
60
40
20
0
cnt
100
1000
10000
Concentration (nM)

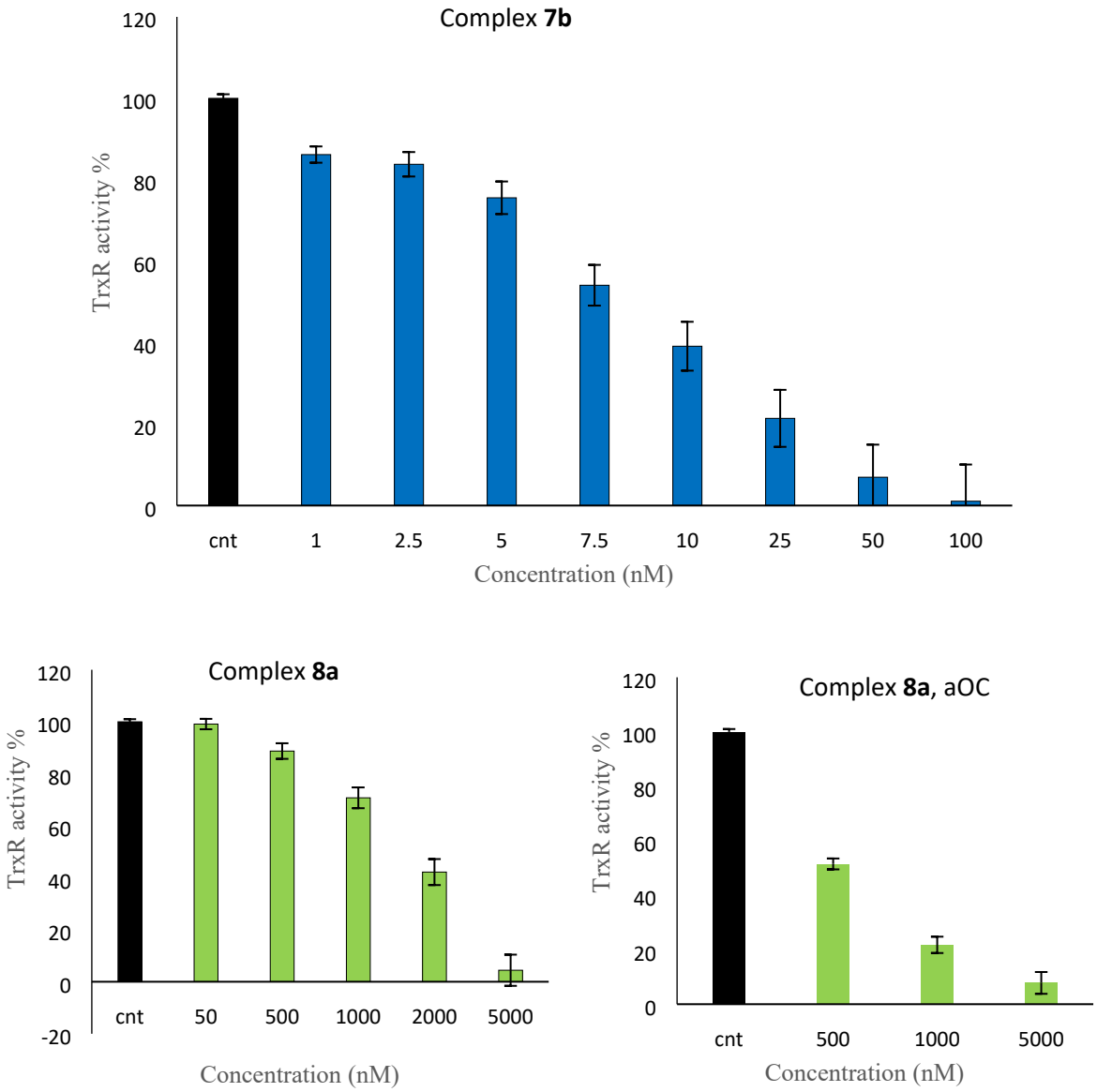

Figure S7. The inhibitory effect of complexes **1a**, **1a-Me**, **2–4a/b**, **5a**, **6–7a/b**, and **8a** on TrxR activity was evaluated under normal and oxidizing conditions (the latter induced by treatment with H_2O_2/HRP, referred to as aOC). The enzyme was incubated with increasing concentrations of the metal complexes, and enzymatic activity was assessed spectrophotometrically, as described in the Materials and Methods section. Where indicated, the compounds were incubated in 0.2 M Tris–HCl buffer (pH 8.1) containing 1 mM EDTA, 22 nM HRP, and 0.1 mM H_2O_2 for 15 min at 25 °C. The mixture was subsequently incubated with TrxR1, and enzymatic activity was measured. Mean values ± SD of 3 independent experiments are reported.

NMR spectra

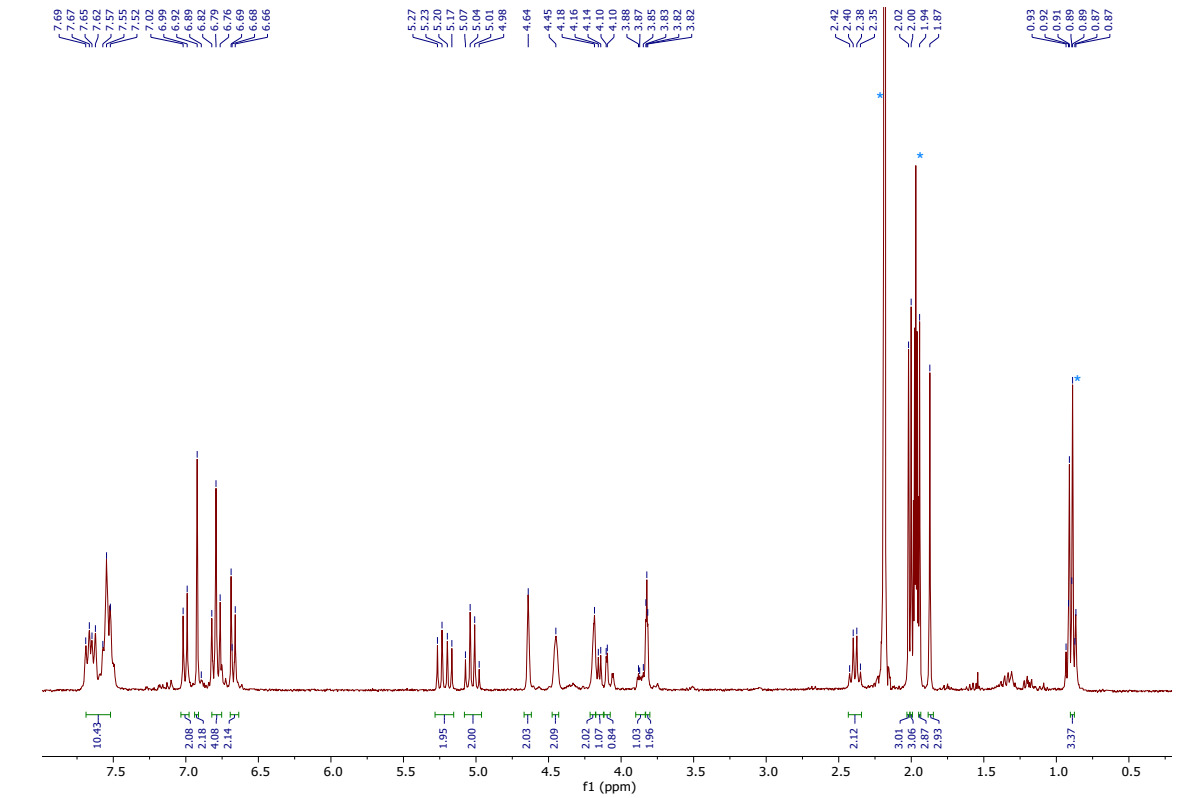

Figure S8. ^{1}H NMR spectrum (300 MHz, CD_3CN) of **3a**.

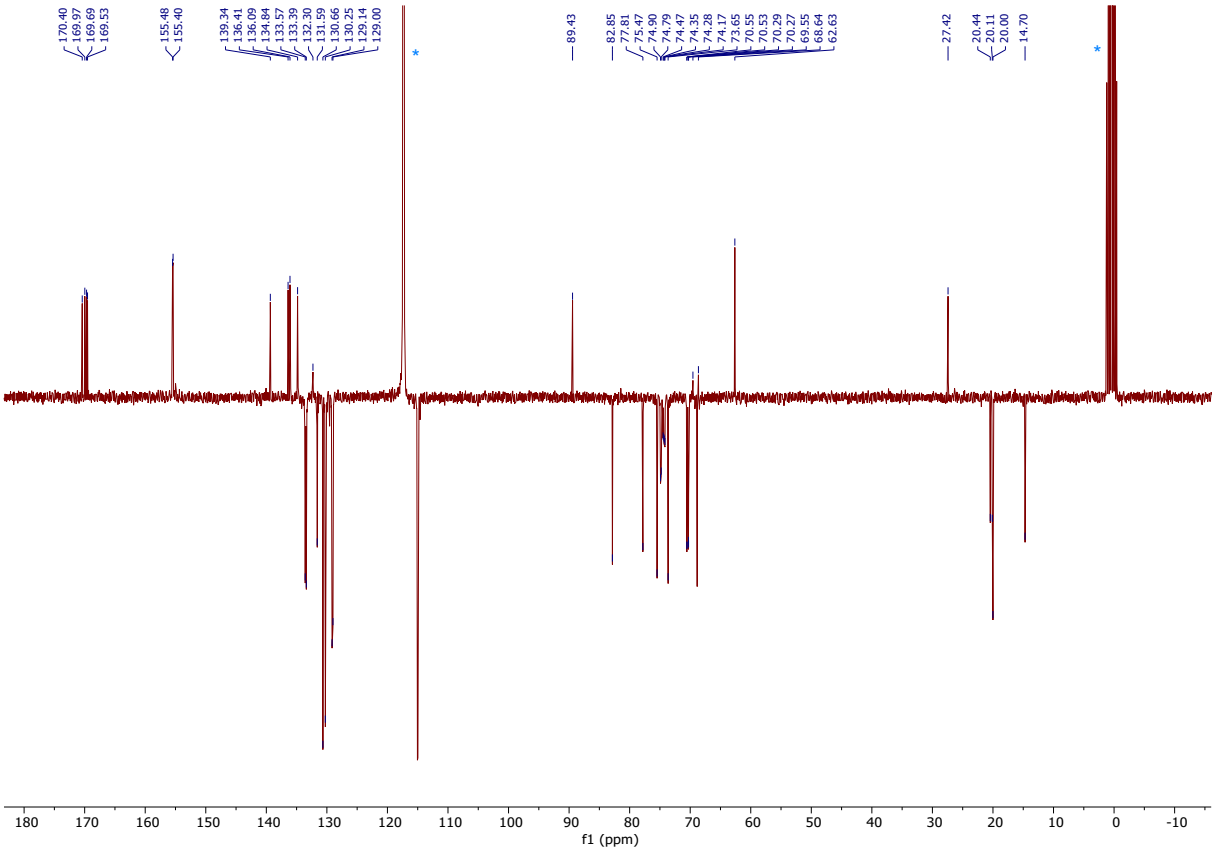

Figure S9. $^{13}C\{^{1}H\}$ NMR spectrum (75 MHz, CD_3CN) of **3a**

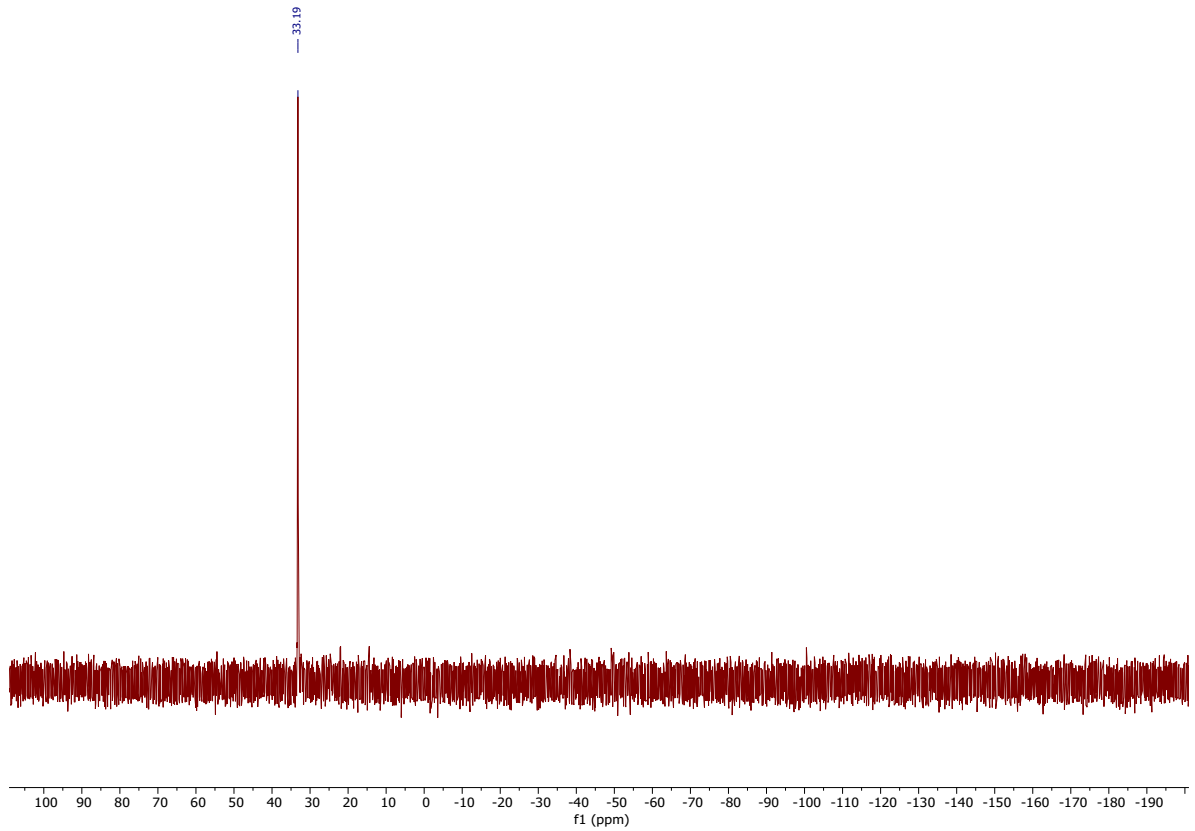

Figure S10. $^{31}P\{^{1}H\}$ NMR spectrum (122 MHz, CD_3CN) of **3a**

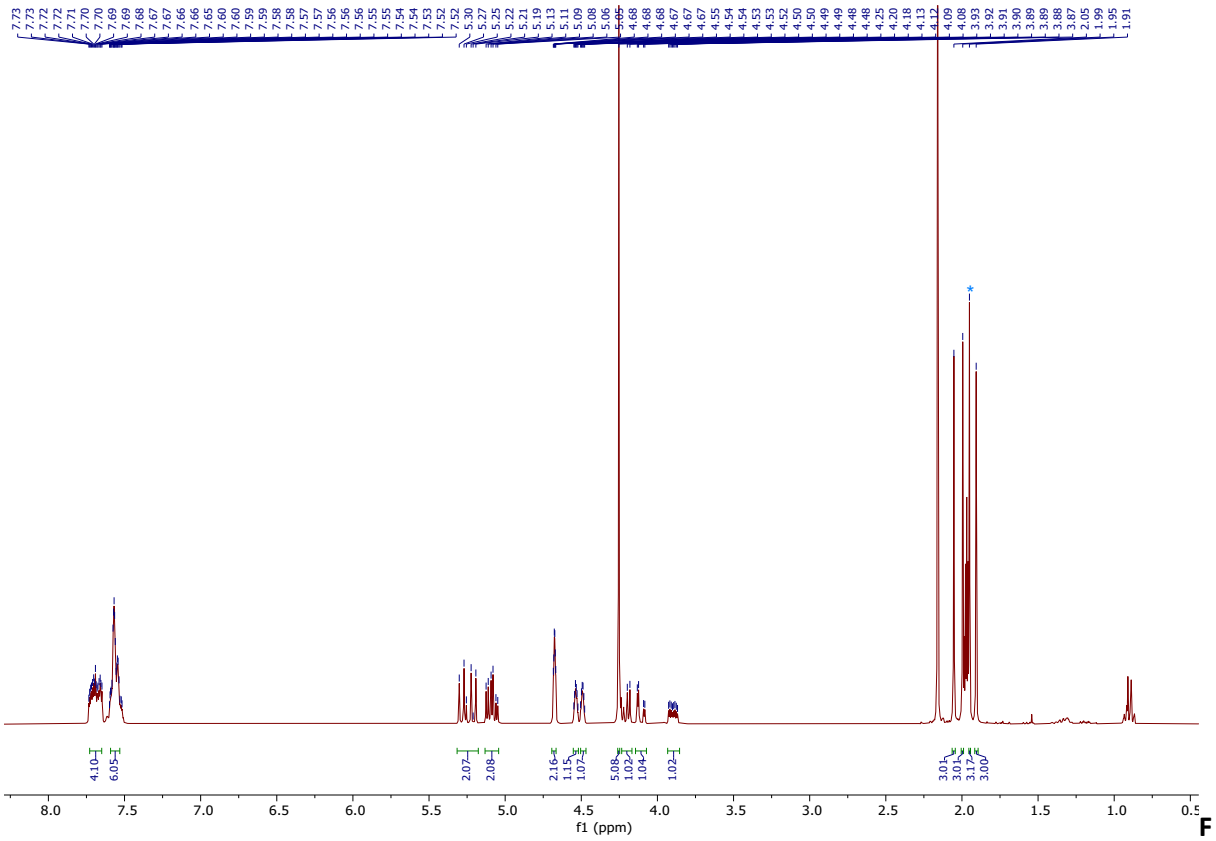

igure S11. ^{1}H NMR spectrum (300 MHz, CD_3CN) of **3b**

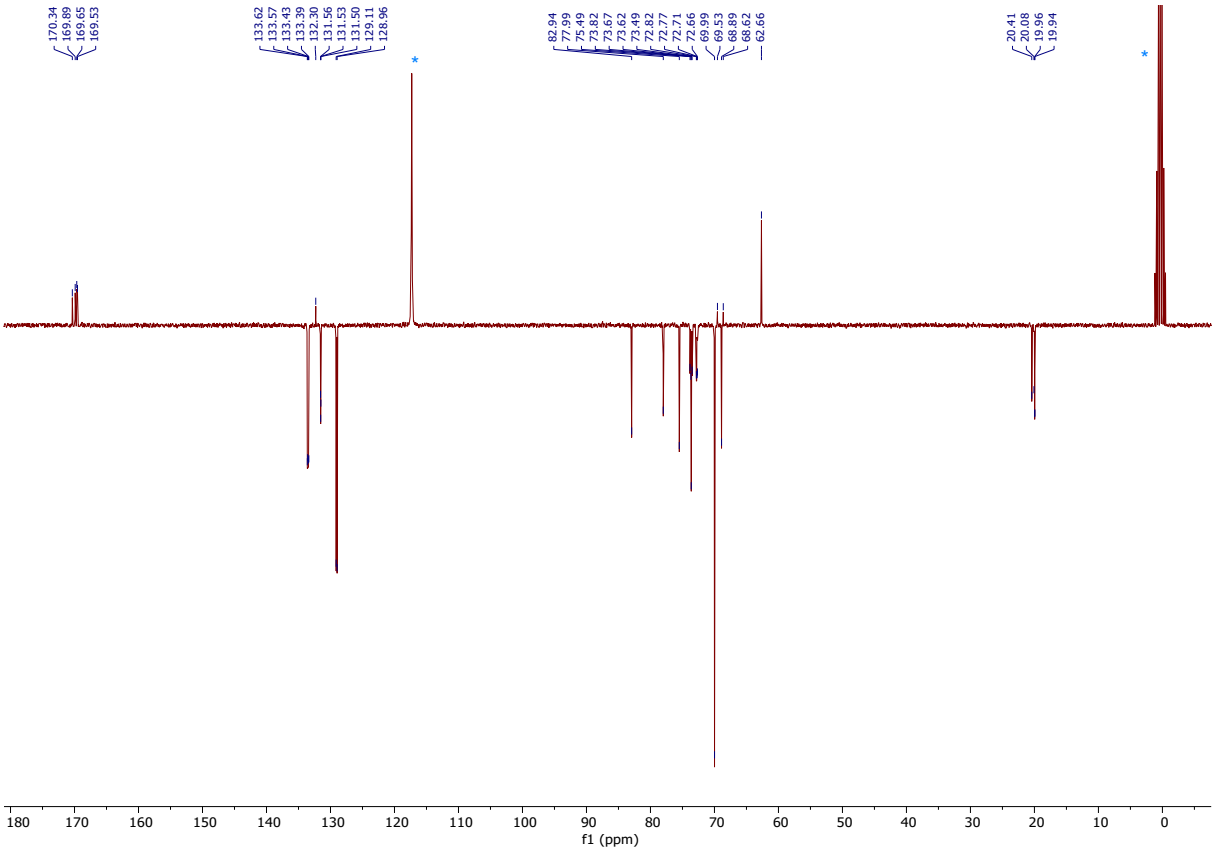

Figure S12. $^{13}C\{^{1}H\}$ NMR spectrum (75 MHz, CD_3CN) of **3b**

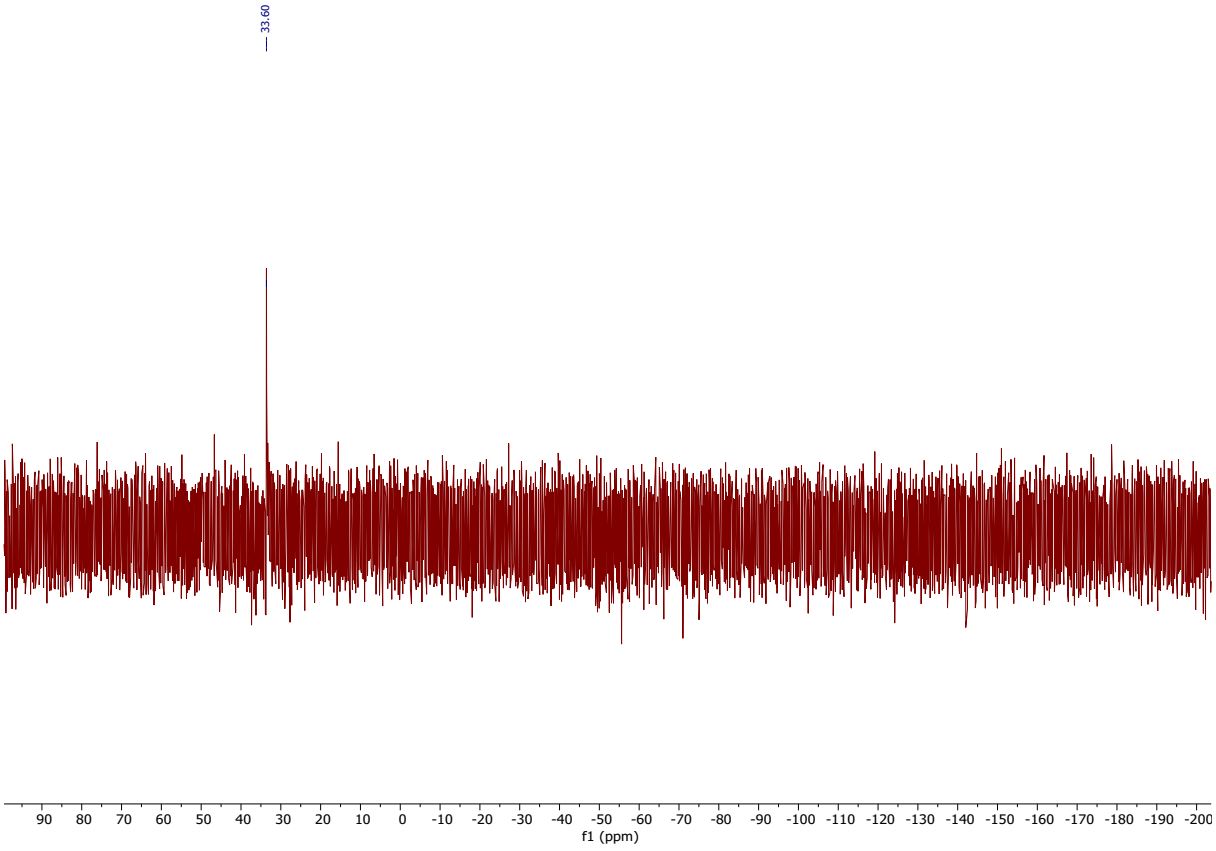

Figure S13. $^{31}P\{^{1}H\}$ NMR spectrum (122 MHz, CD_3CN) of **3b**

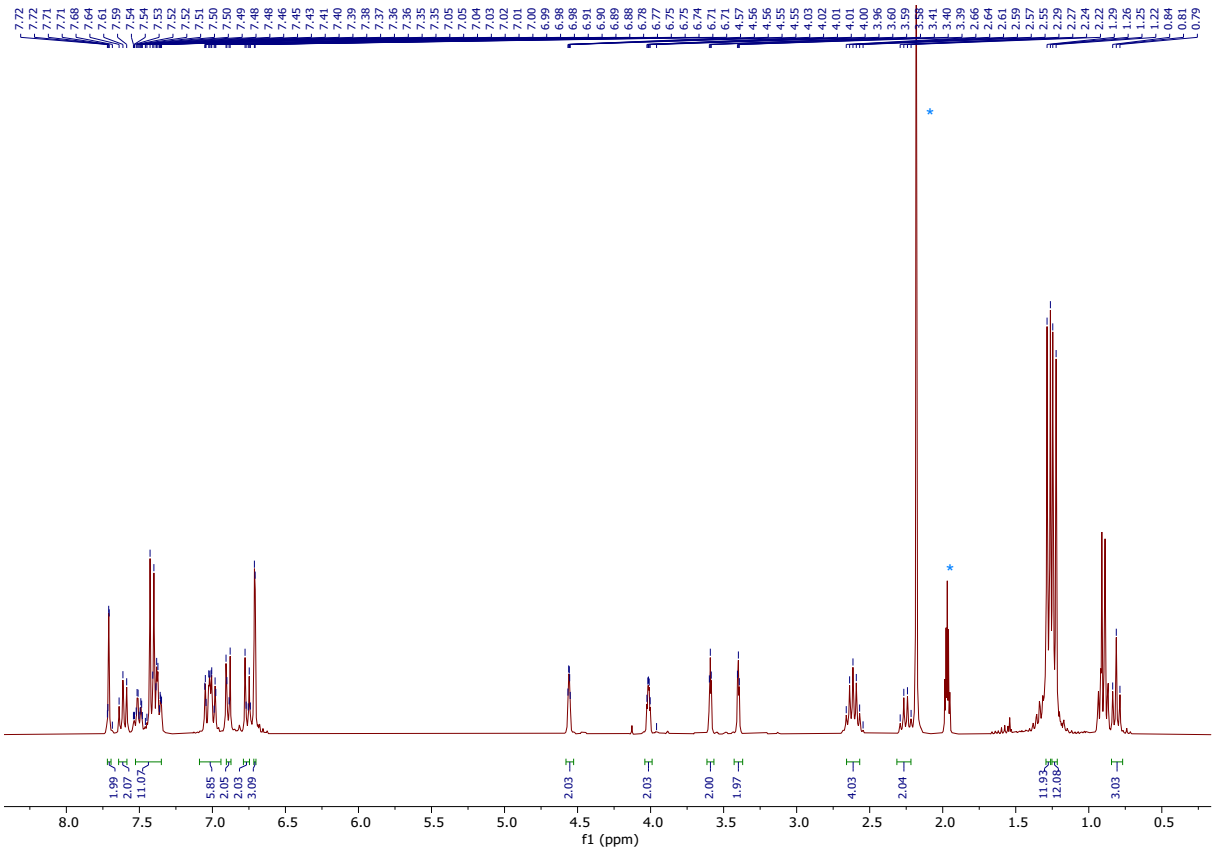

Figure S14. ^{1}H NMR spectrum (300 MHz, CD_3CN) of **4a**

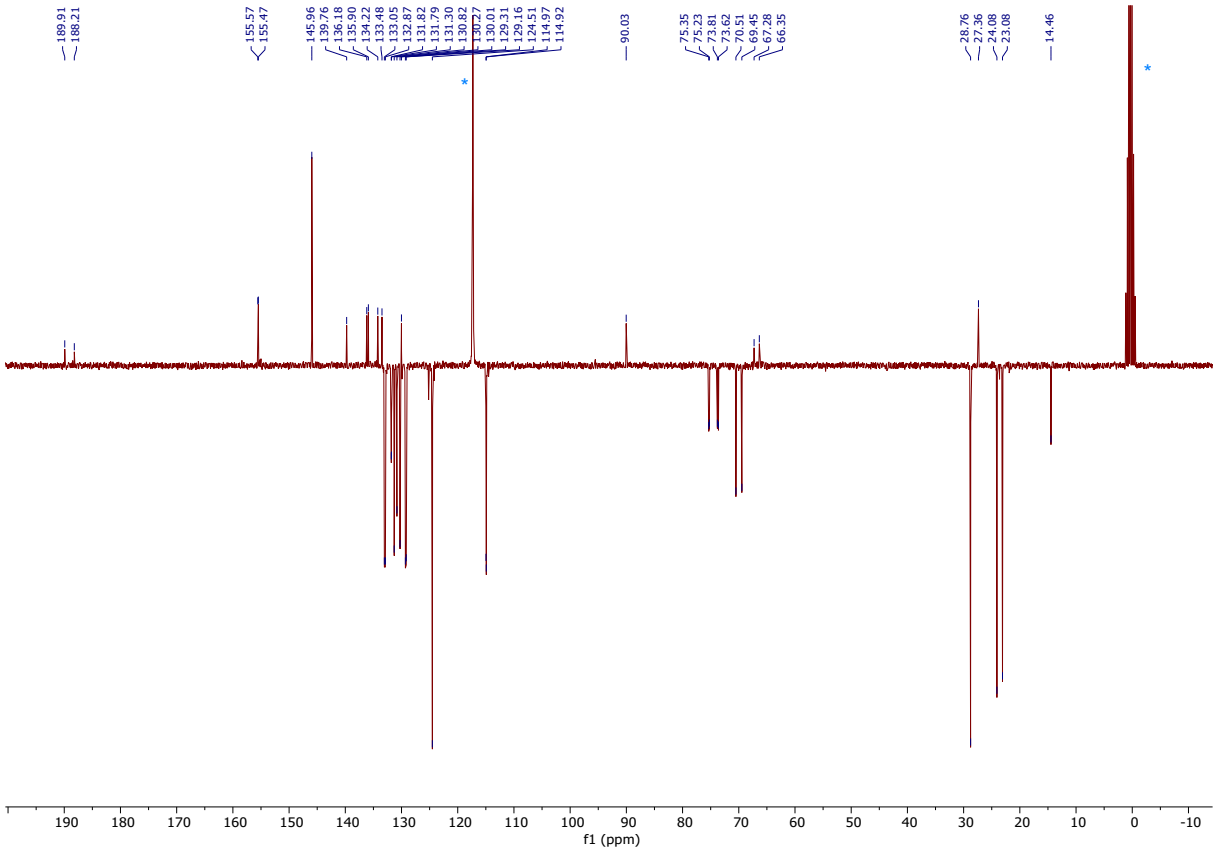

Figure S15. $^{13}C\{^{1}H\}$ NMR spectrum (75 MHz, CD_3CN) of **4a**

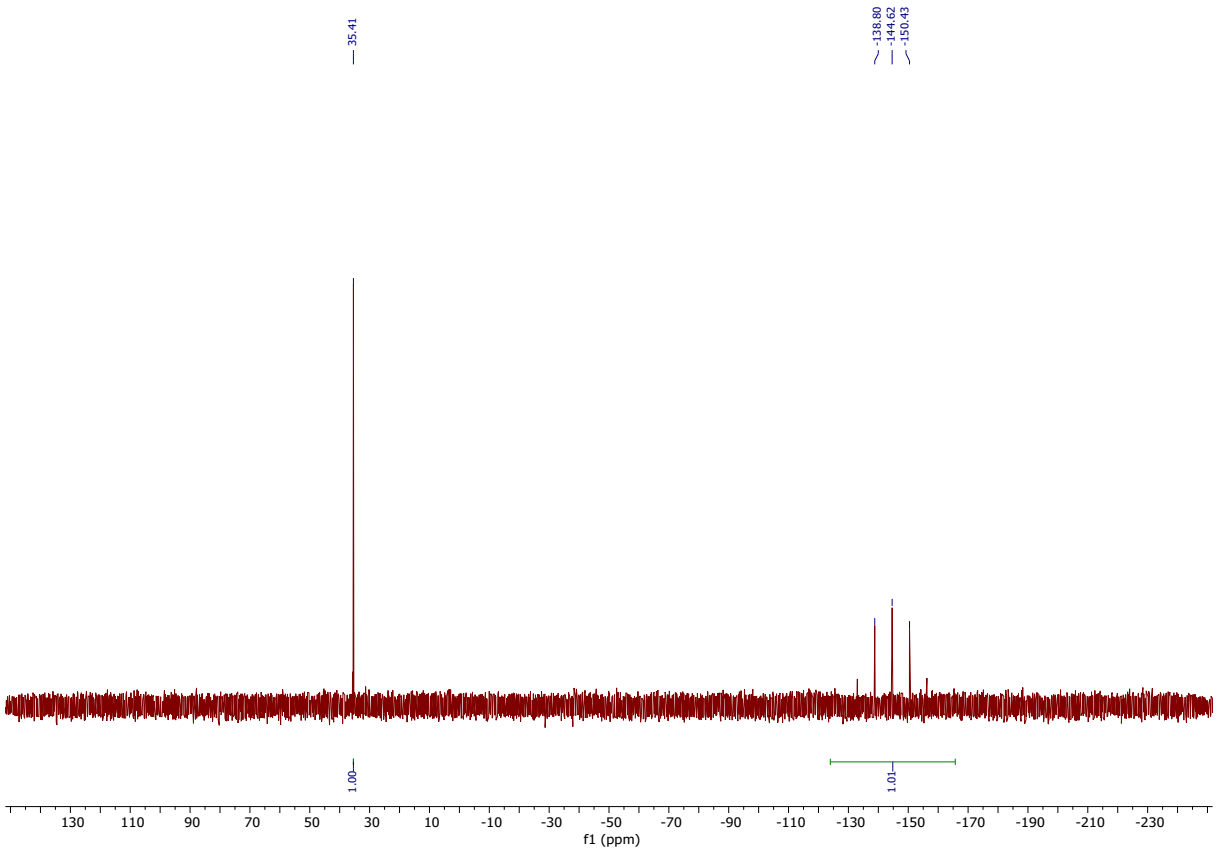

Figure S16. $^{31}P\{^{1}H\}$ NMR spectrum (122 MHz, CD_3CN) of **4a**

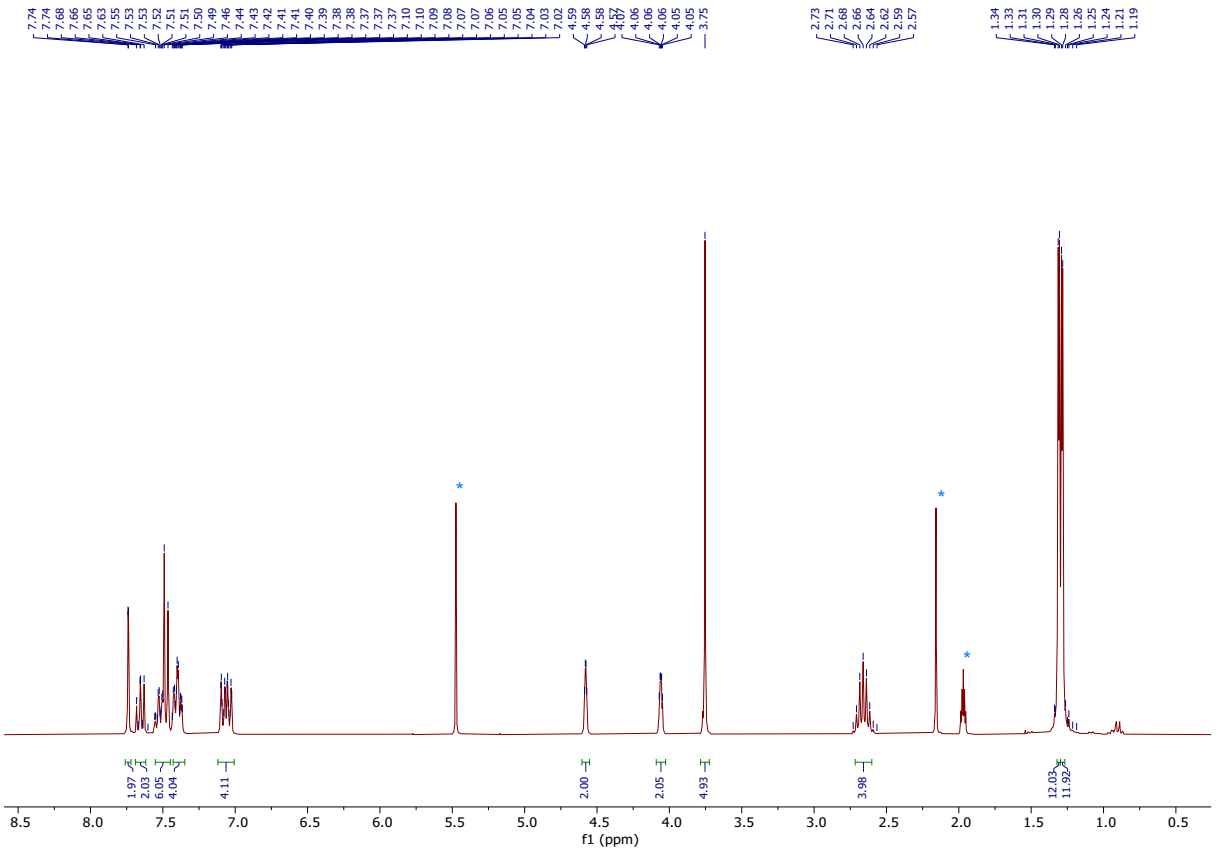

Figure S17. ^{1}H NMR spectrum (300 MHz, CD_3CN) of **4b**.

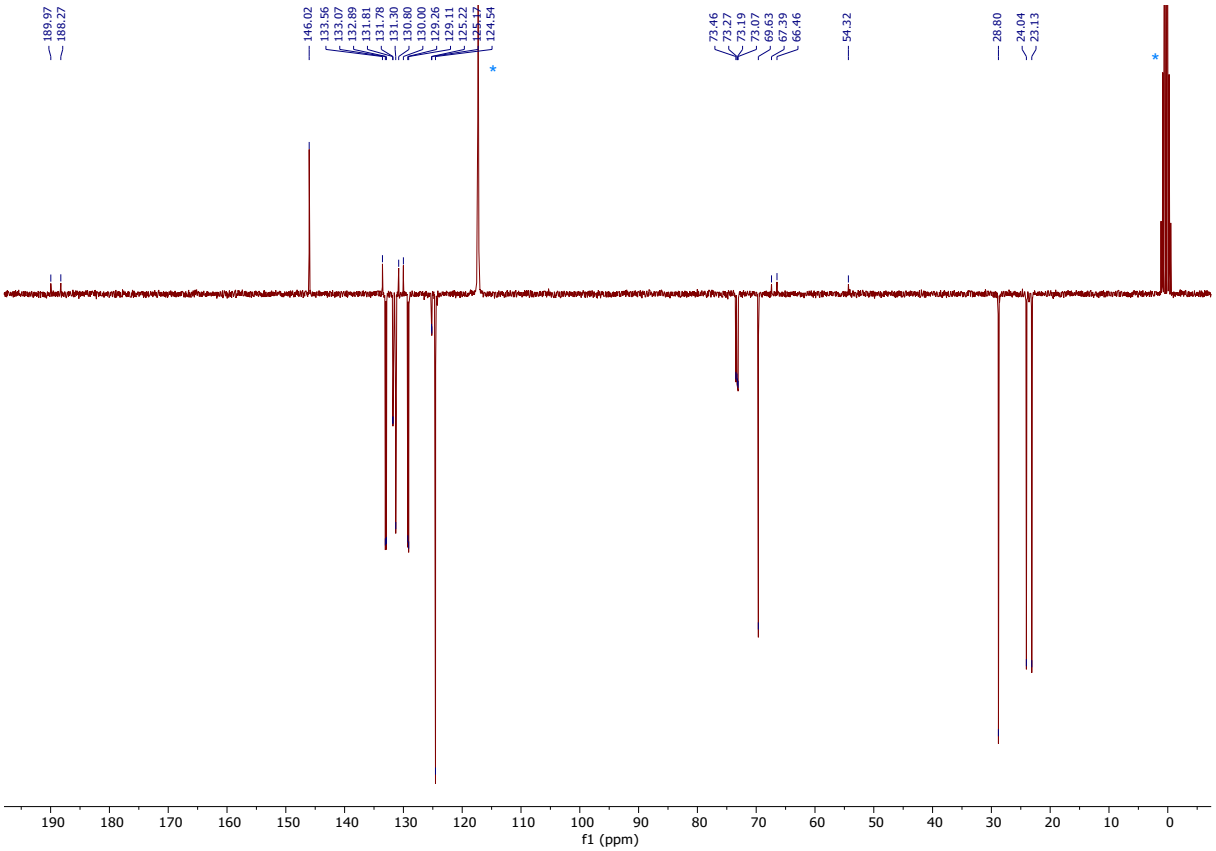

Figure S18. $^{13}C\{^{1}H\}$ NMR spectrum (75 MHz, CD_3CN) of **4b**

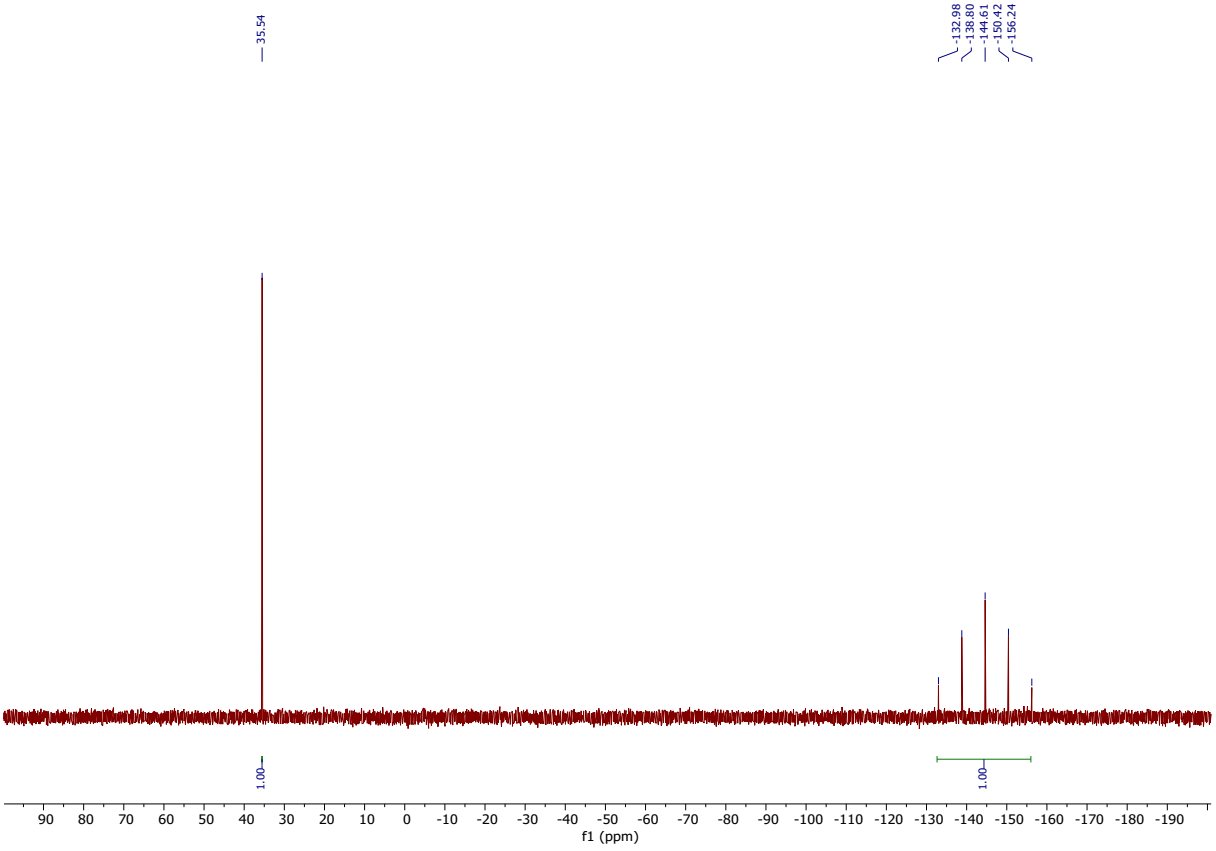

Figure S19. $^{31}P\{^{1}H\}$ NMR spectrum (122 MHz, CD_3CN) of **4b**

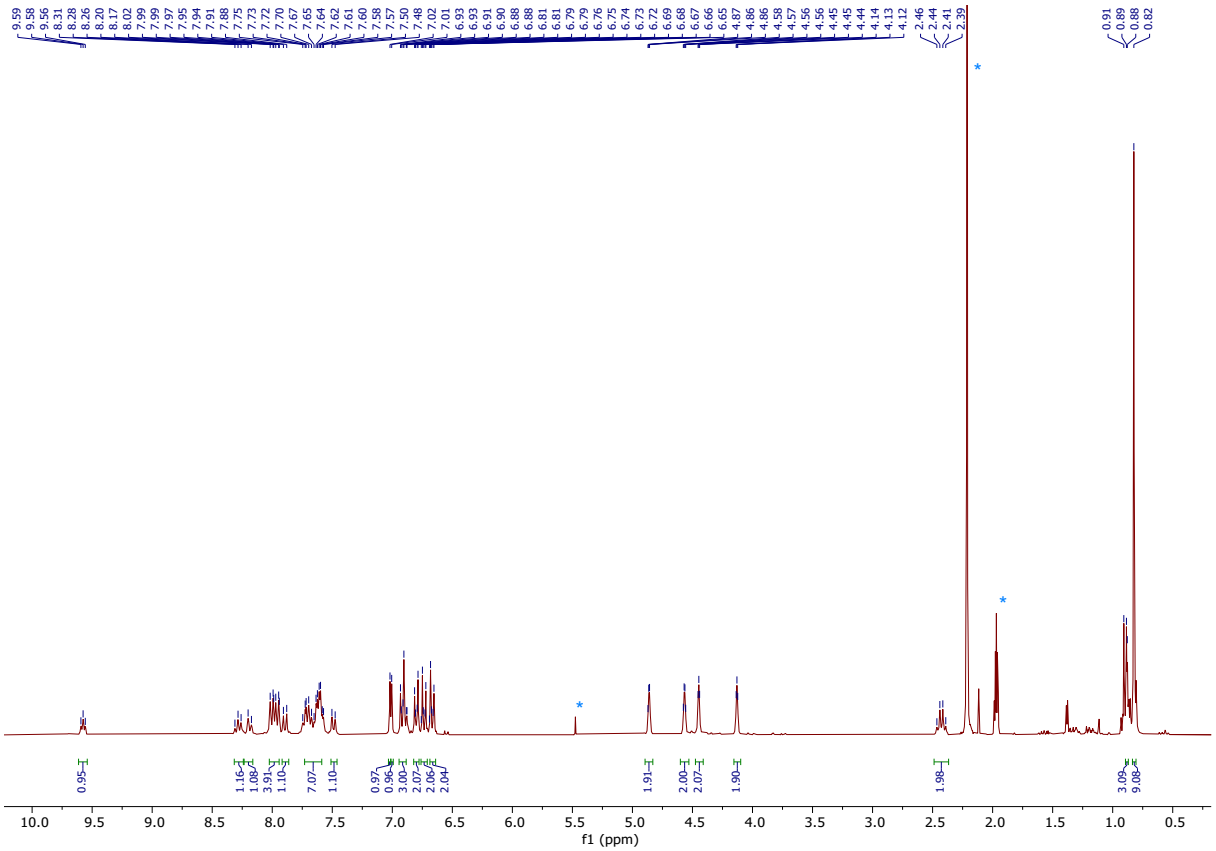

Figure S20. ^{1}H NMR spectrum (300 MHz, CD_3CN) of **5a**

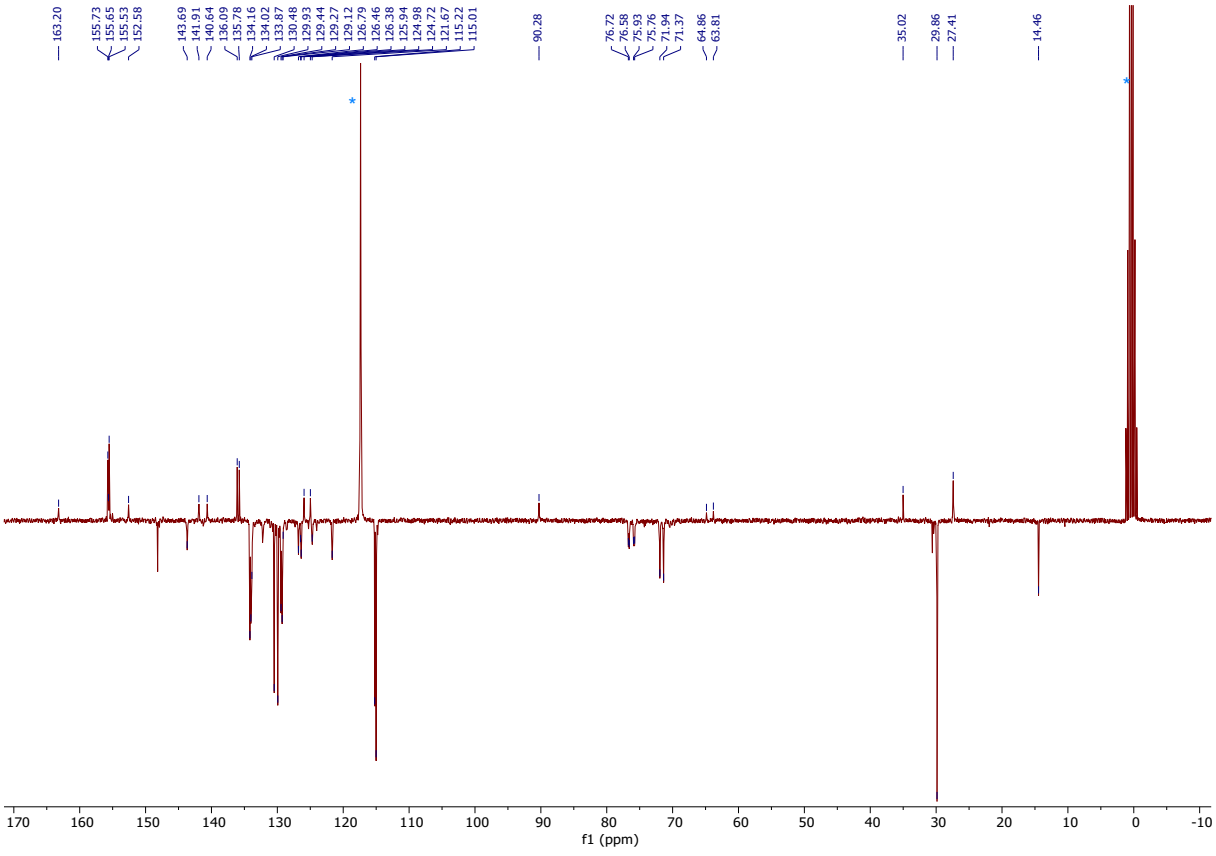

Figure S21. $^{13}C\{^{1}H\}$ NMR spectrum (75 MHz, CD_3CN) of **5a**

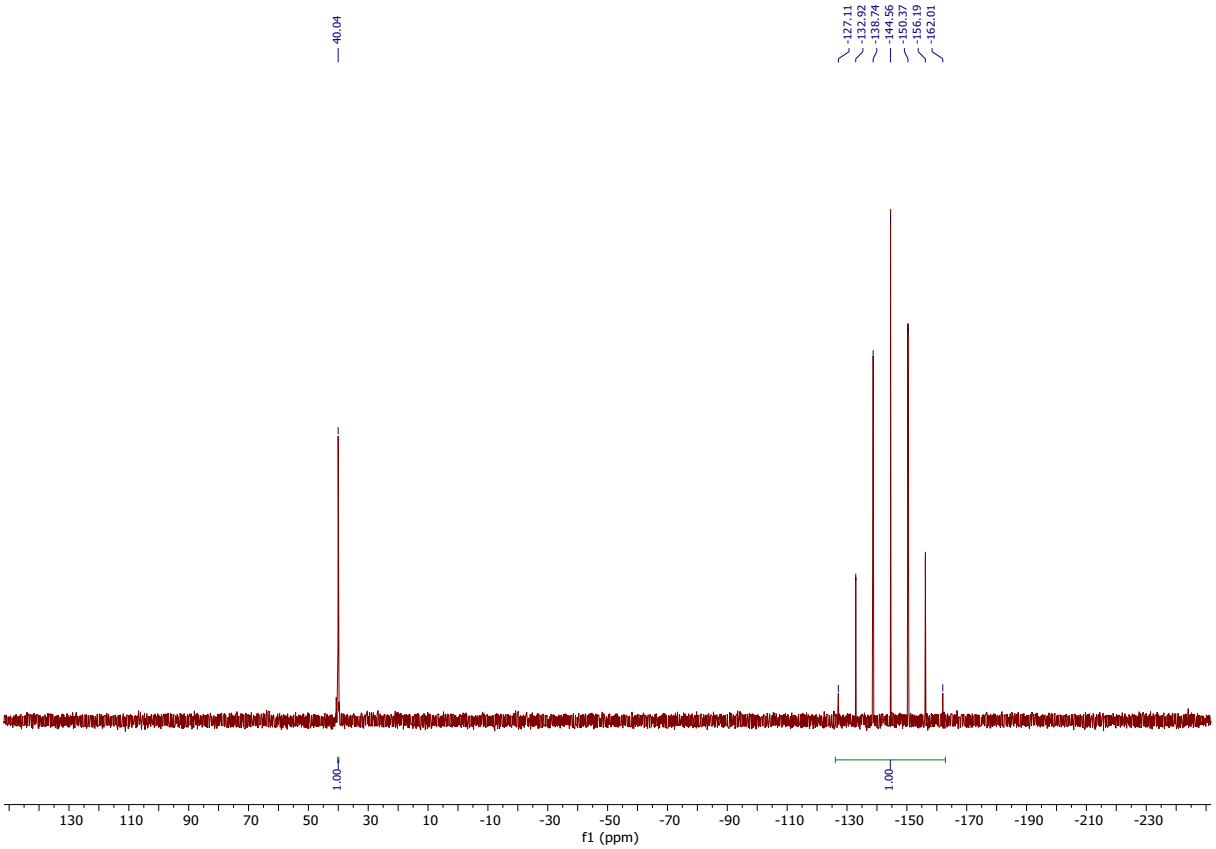

Figure S22. $^{31}P\{^{1}H\}$ NMR spectrum (122 MHz, CD_3CN) of **5a**

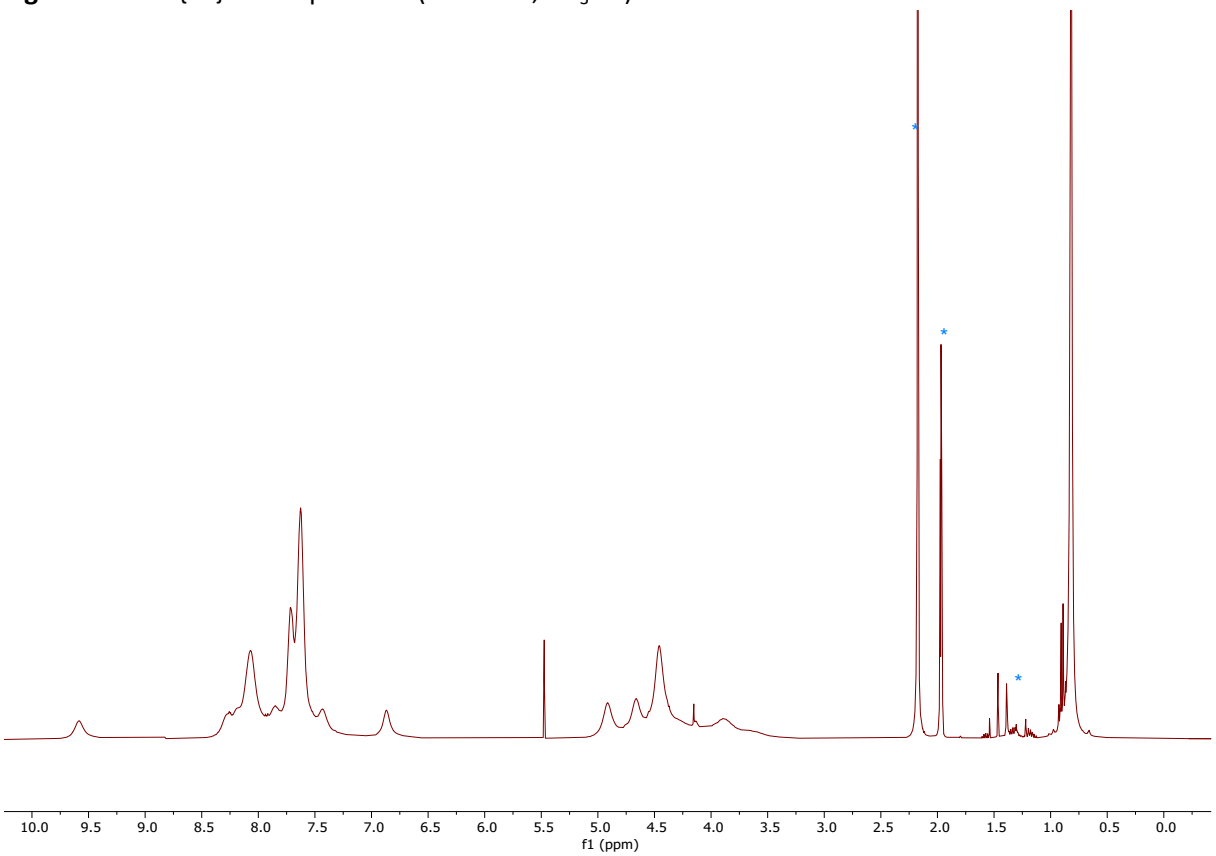

Figure S23. ^{1}H NMR spectrum (300 MHz, CD_3CN) of **5b**

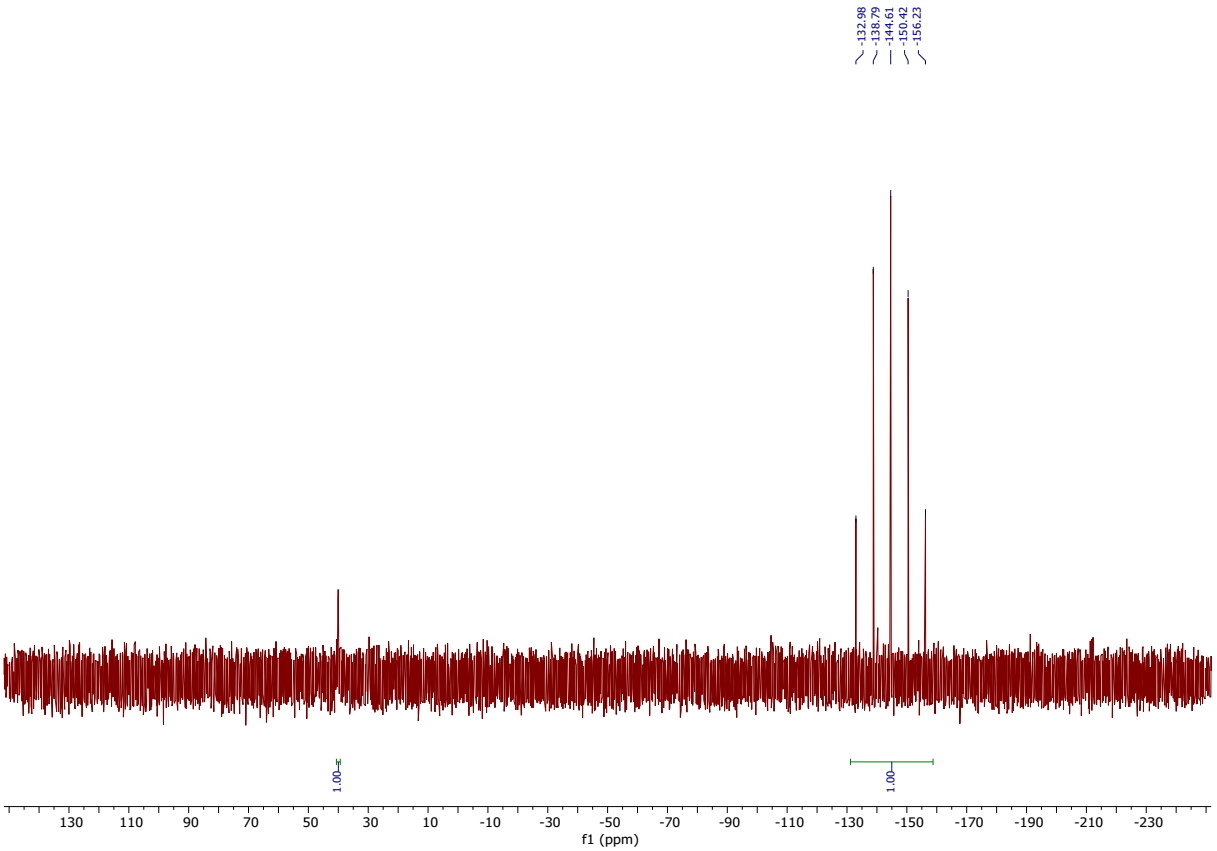

Figure S24. $^{31}P\{^{1}H\}$ NMR spectrum (122 MHz, CD_3CN) of **5b**

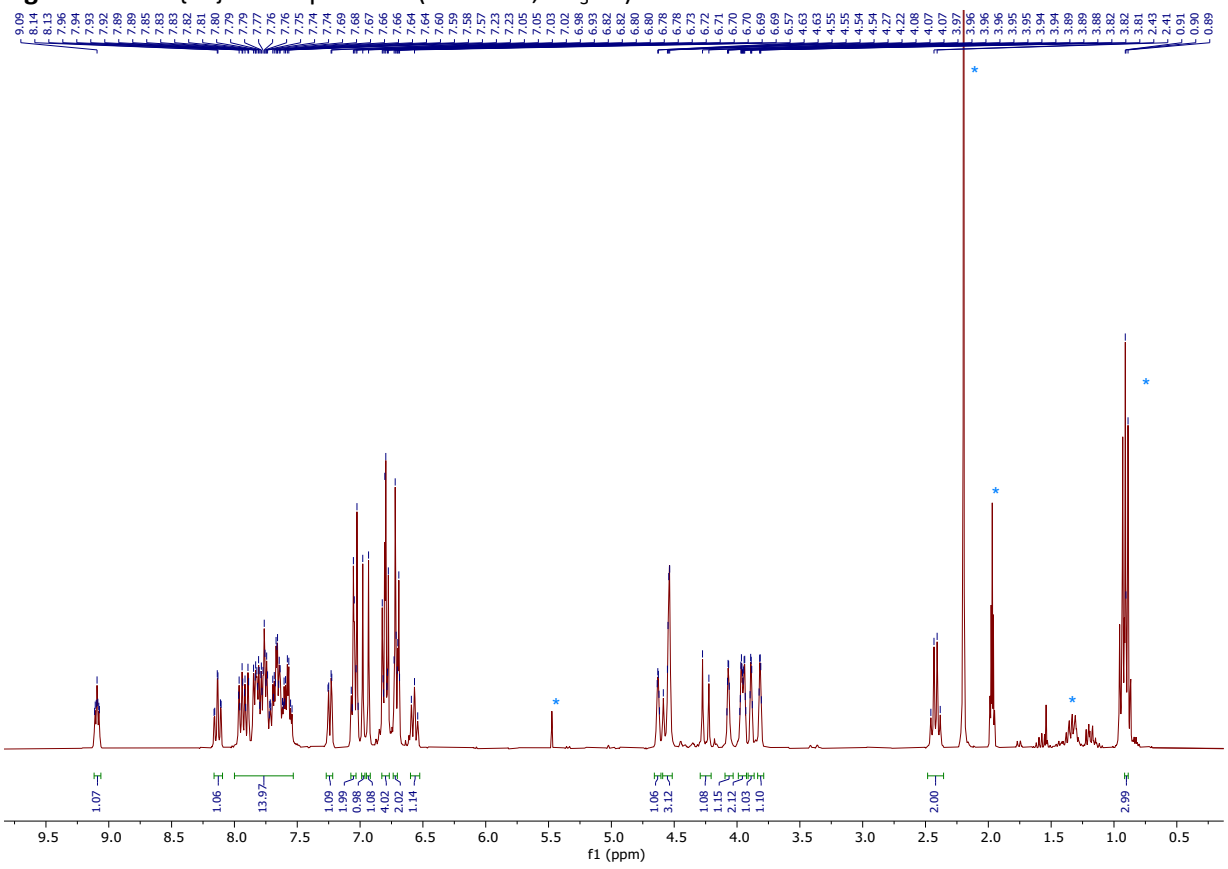

Figure S25. ^{1}H NMR spectrum (300 MHz, CD_3CN) of **6a**

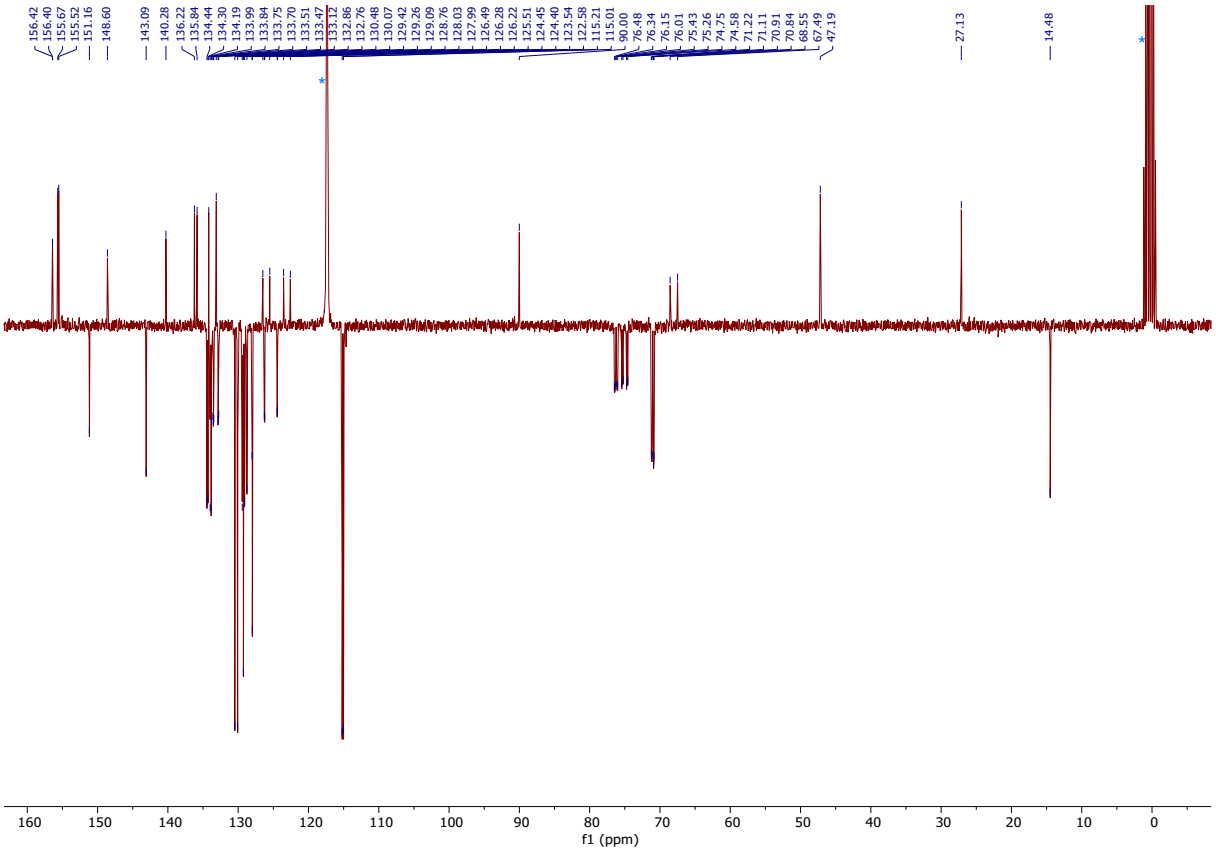

Figure S26. $^{13}C\{^{1}H\}$ NMR spectrum (75 MHz, CD_3CN) of **6a**

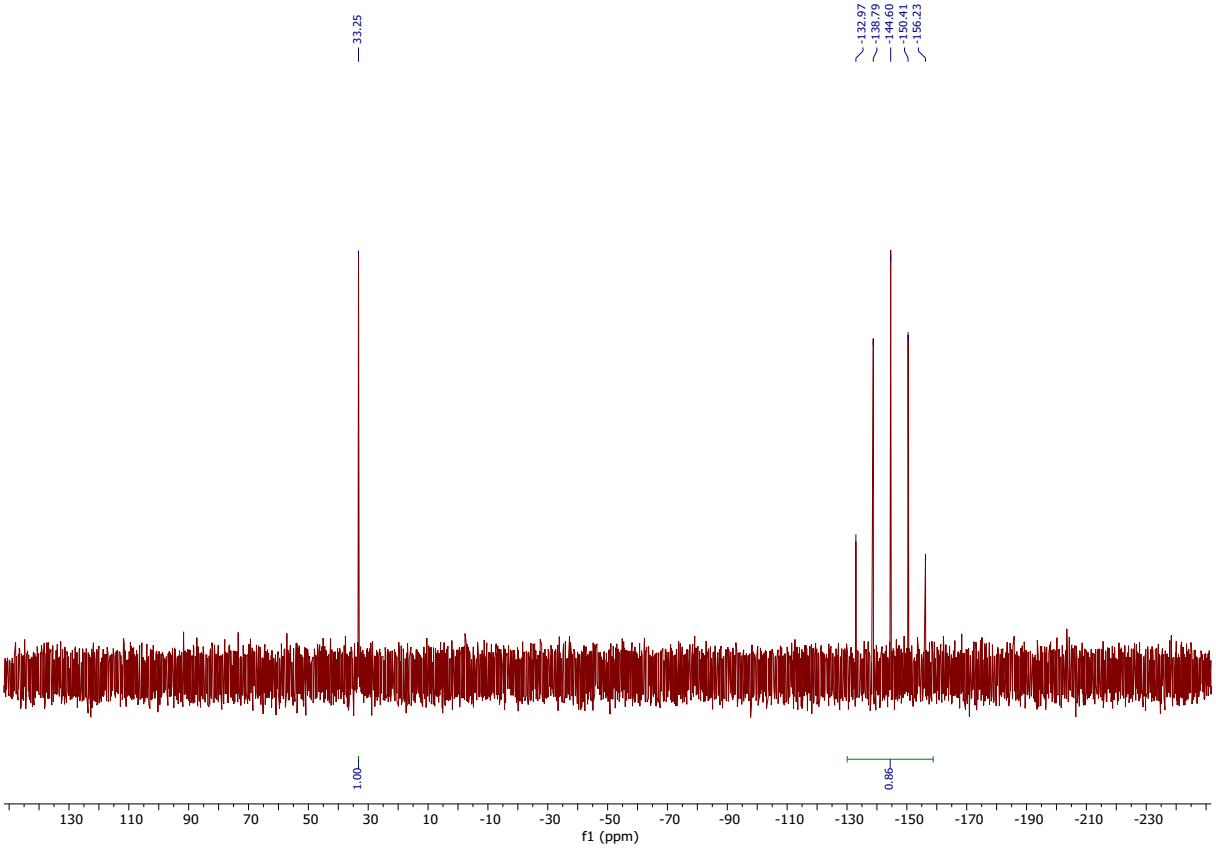

Figure S27. $^{31}P\{^{1}H\}$ NMR spectrum (122 MHz, CD_3CN) of **6a**

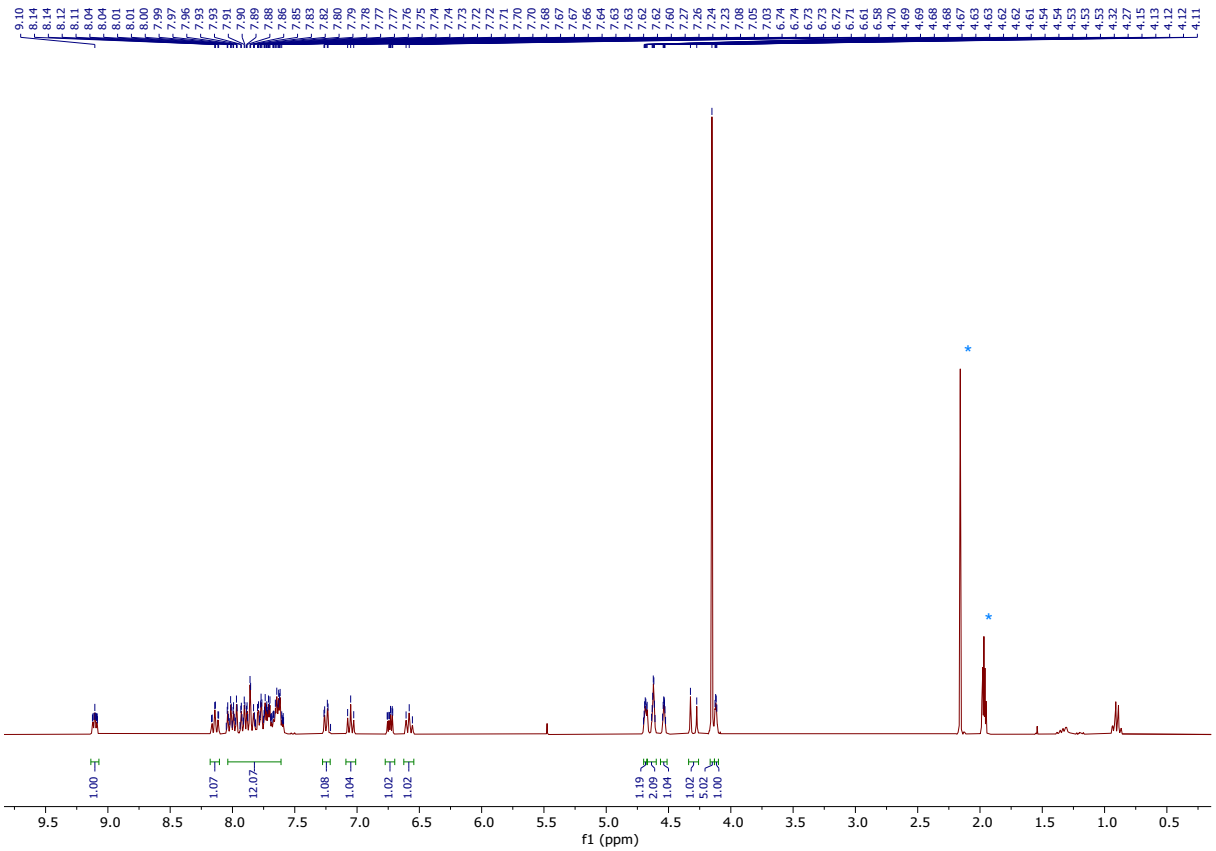

Figure S28. ^{1}H NMR spectrum (300 MHz, CD_3CN) of **6b**

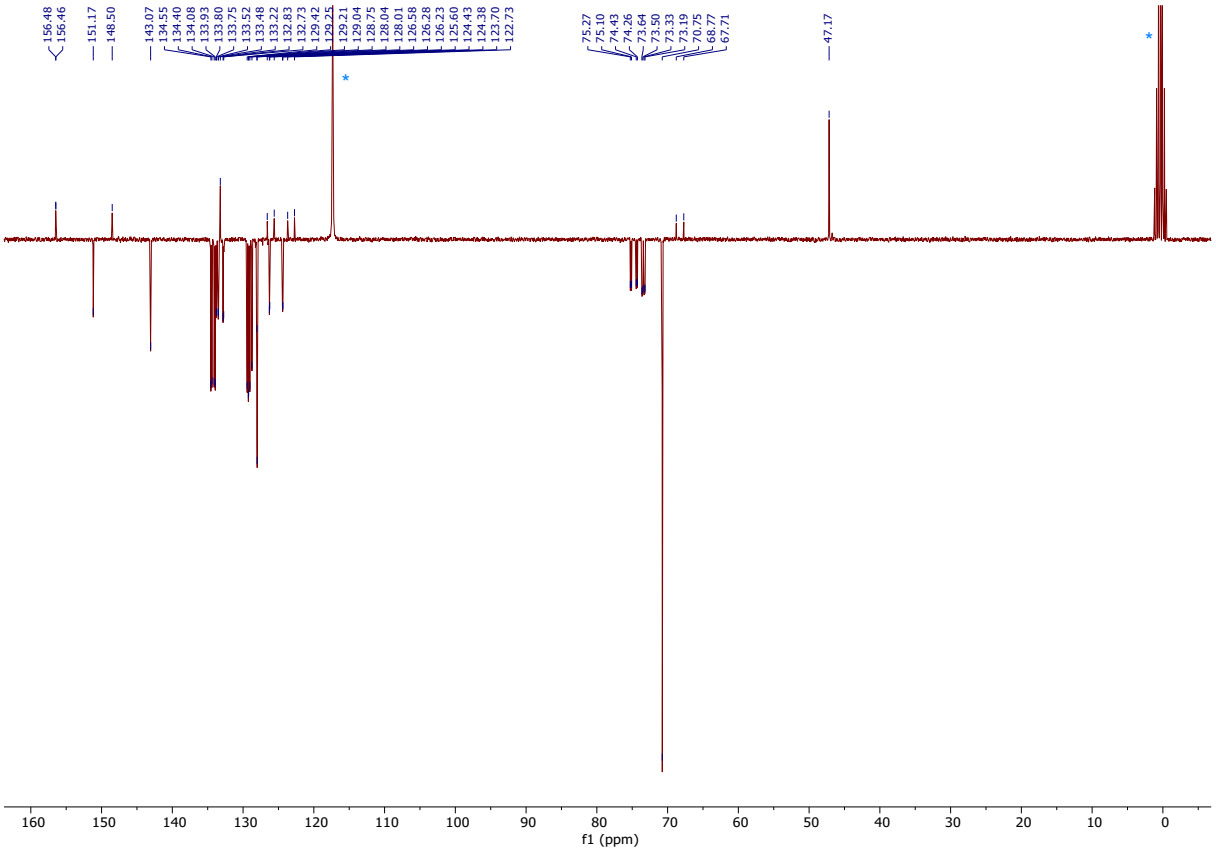

Figure S29. $^{13}C\{^{1}H\}$ NMR spectrum (75 MHz, CD_3CN) of **6b**

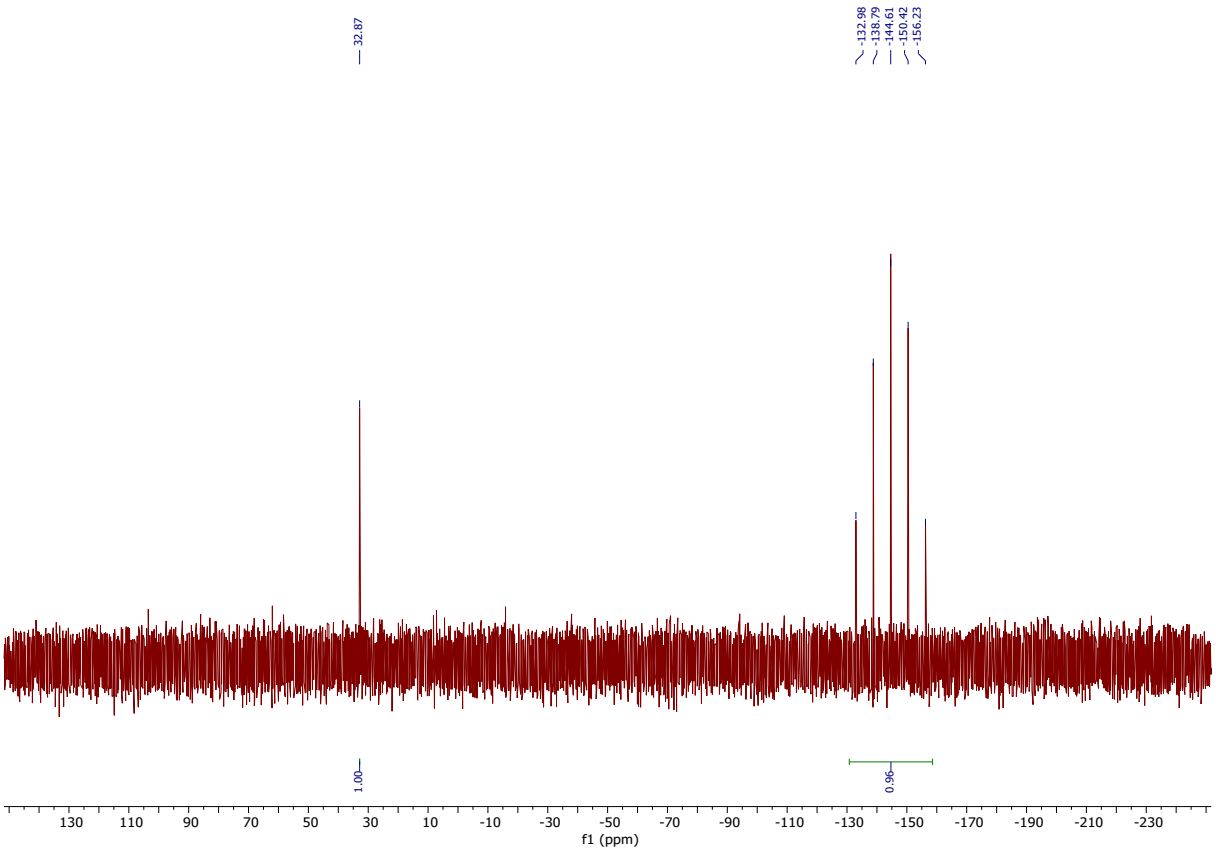

Figure S30. $^{31}P\{^{1}H\}$ NMR spectrum (122 MHz, CD_3CN) of **6b**

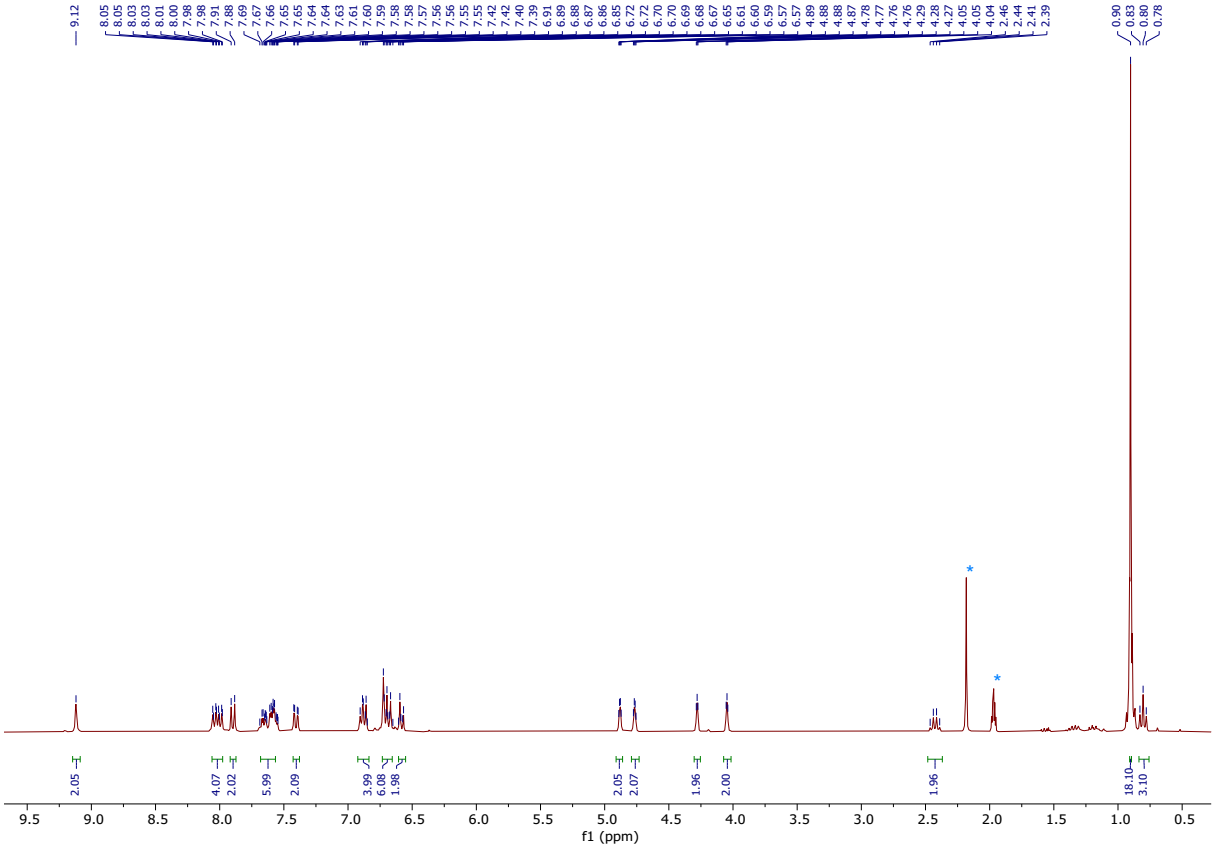

Figure S31. ^{1}H NMR spectrum (300 MHz, CD_3CN) of **7a**

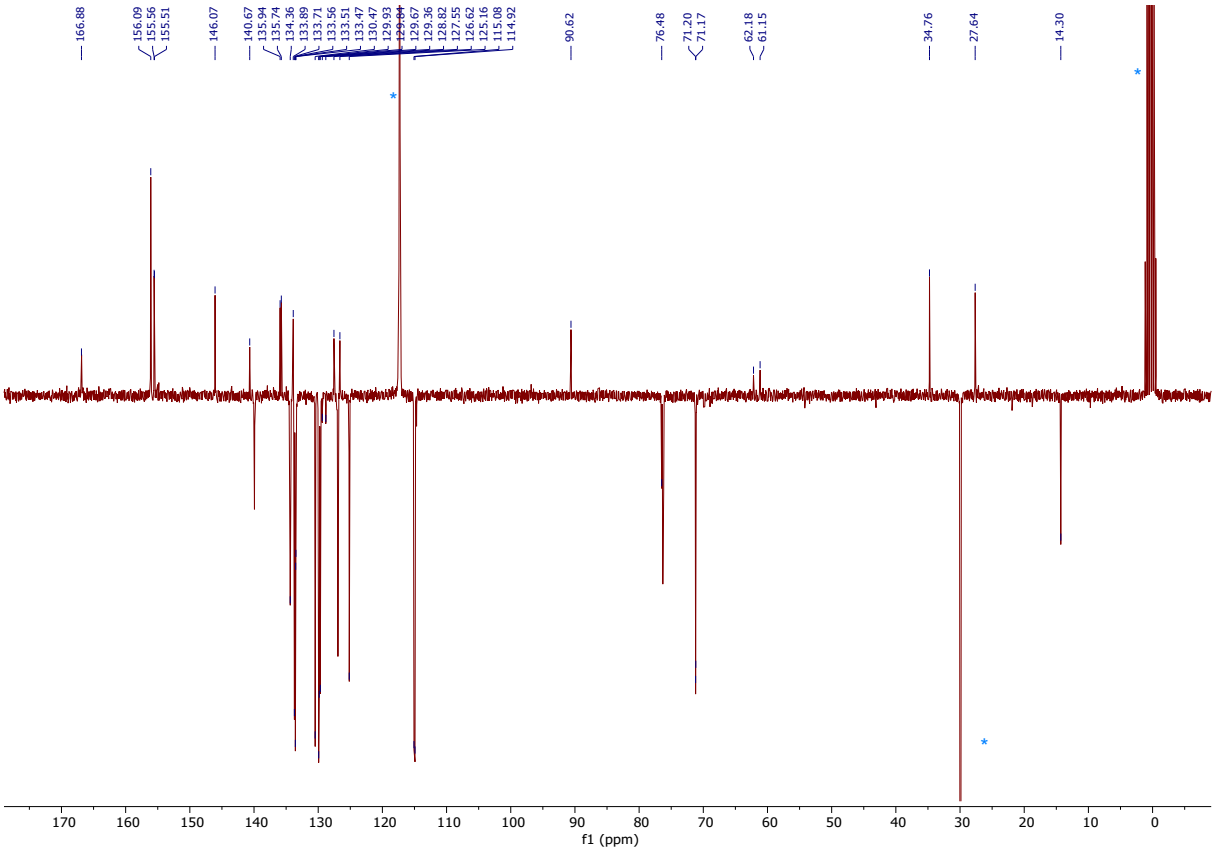

Figure S32. $^{13}C\{^{1}H\}$ NMR spectrum (75 MHz, CD_3CN) of **7a**

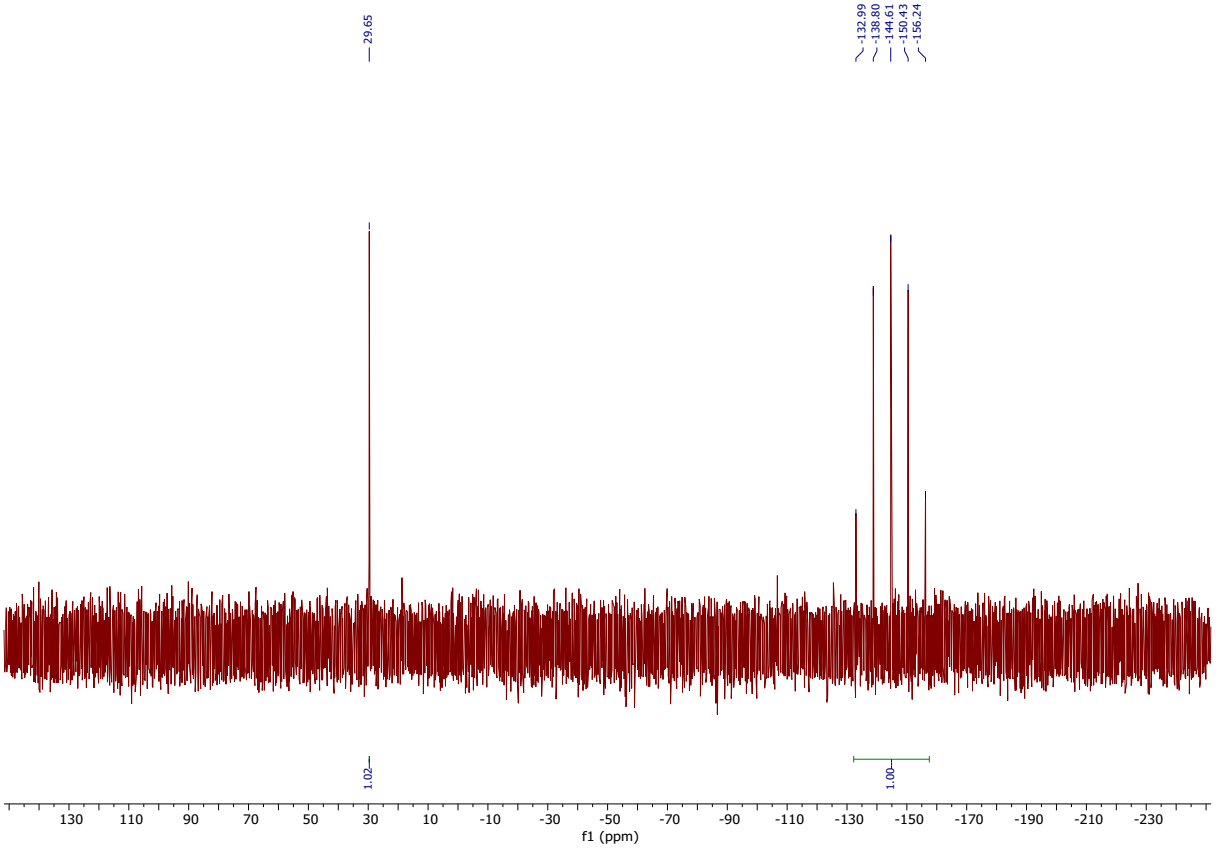

Figure S33. $^{31}P\{^{1}H\}$ NMR spectrum (122 MHz, CD_3CN) of **7a**

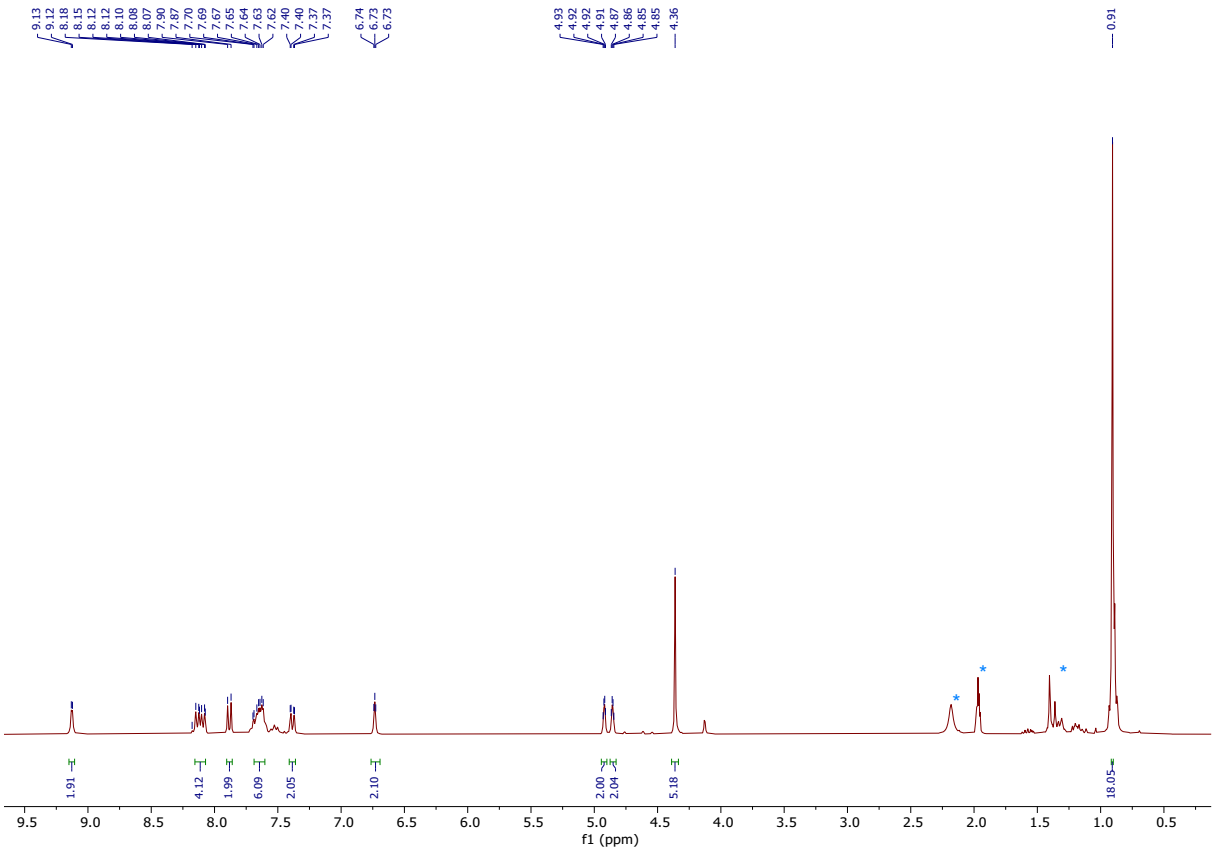

Figure S34. ^{1}H NMR spectrum (300 MHz, CD_3CN) of **7b**

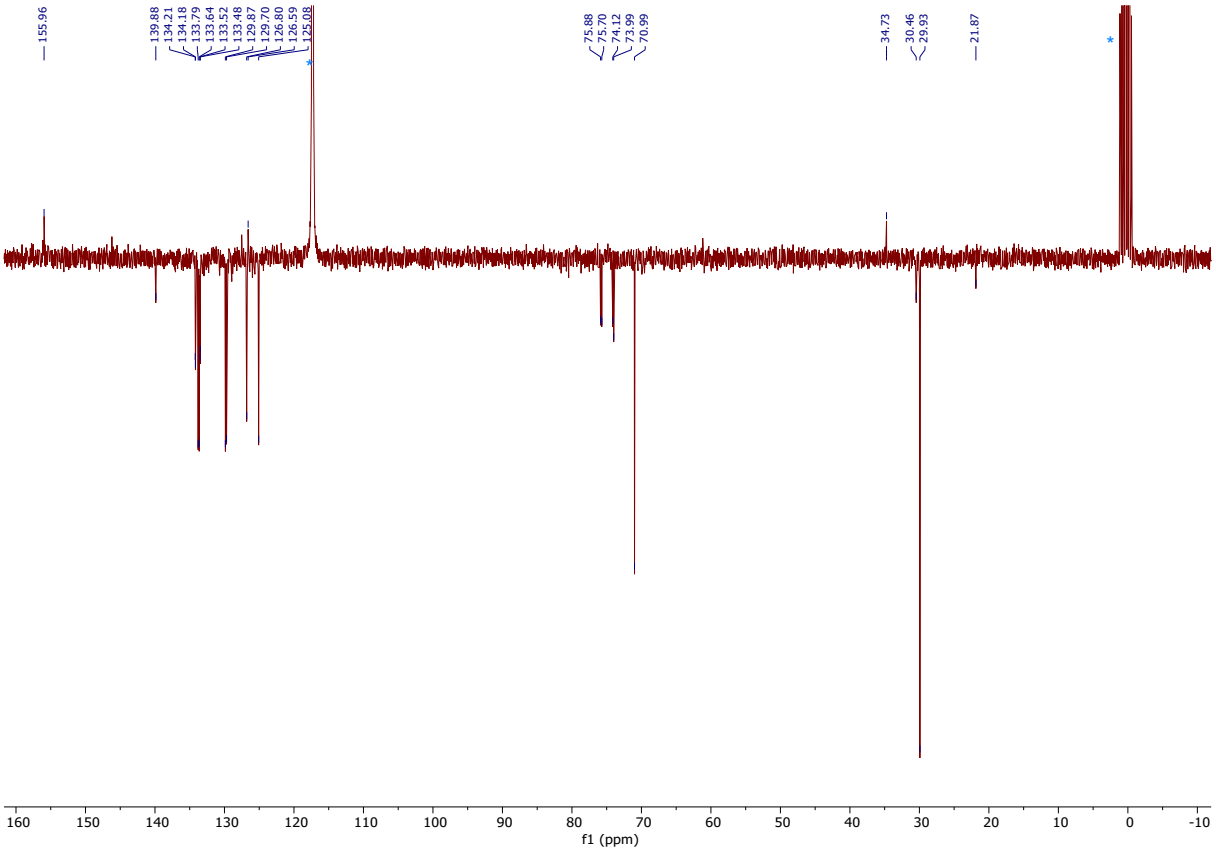

Figure S35. $^{13}C\{^{1}H\}$ NMR spectrum (75 MHz, CD_3CN) of **7b**

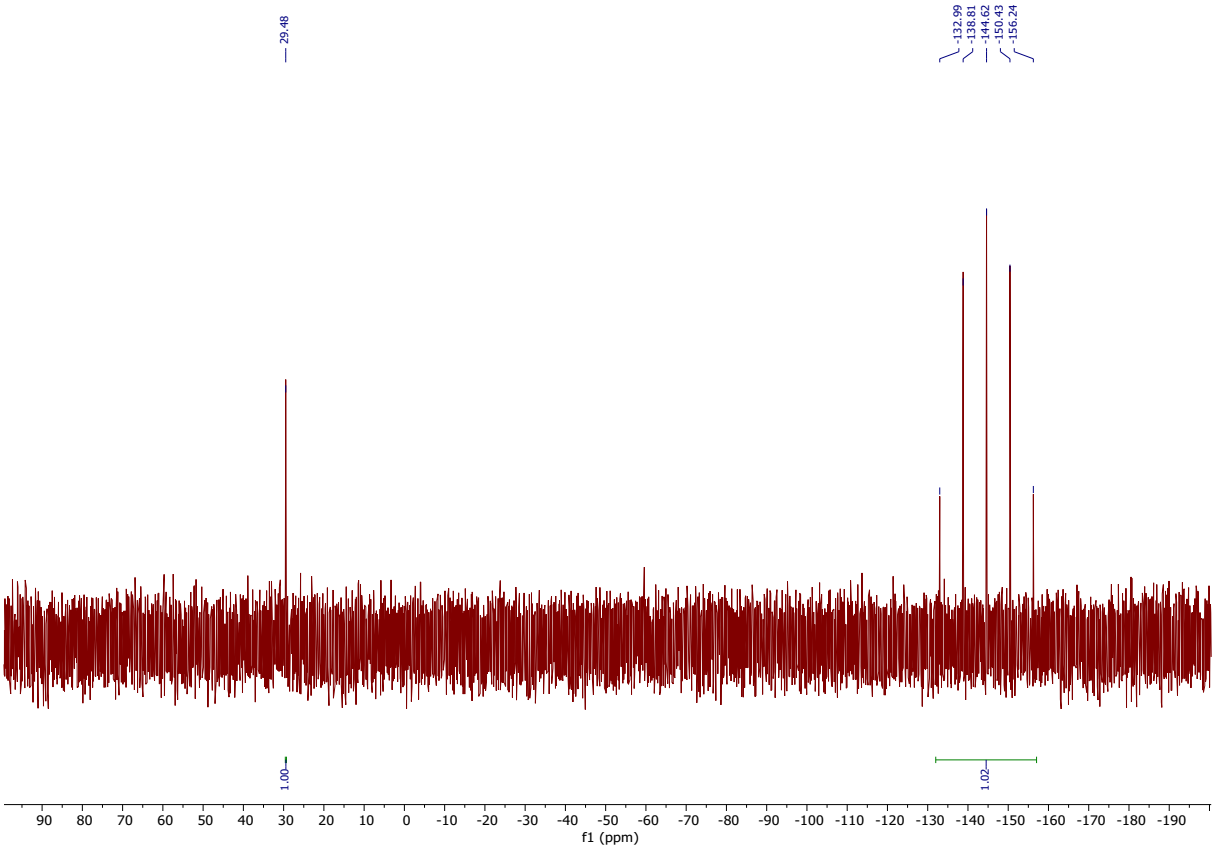

Figure S36. $^{31}P\{^{1}H\}$ NMR spectrum (122 MHz, CD_3CN) of **7b**

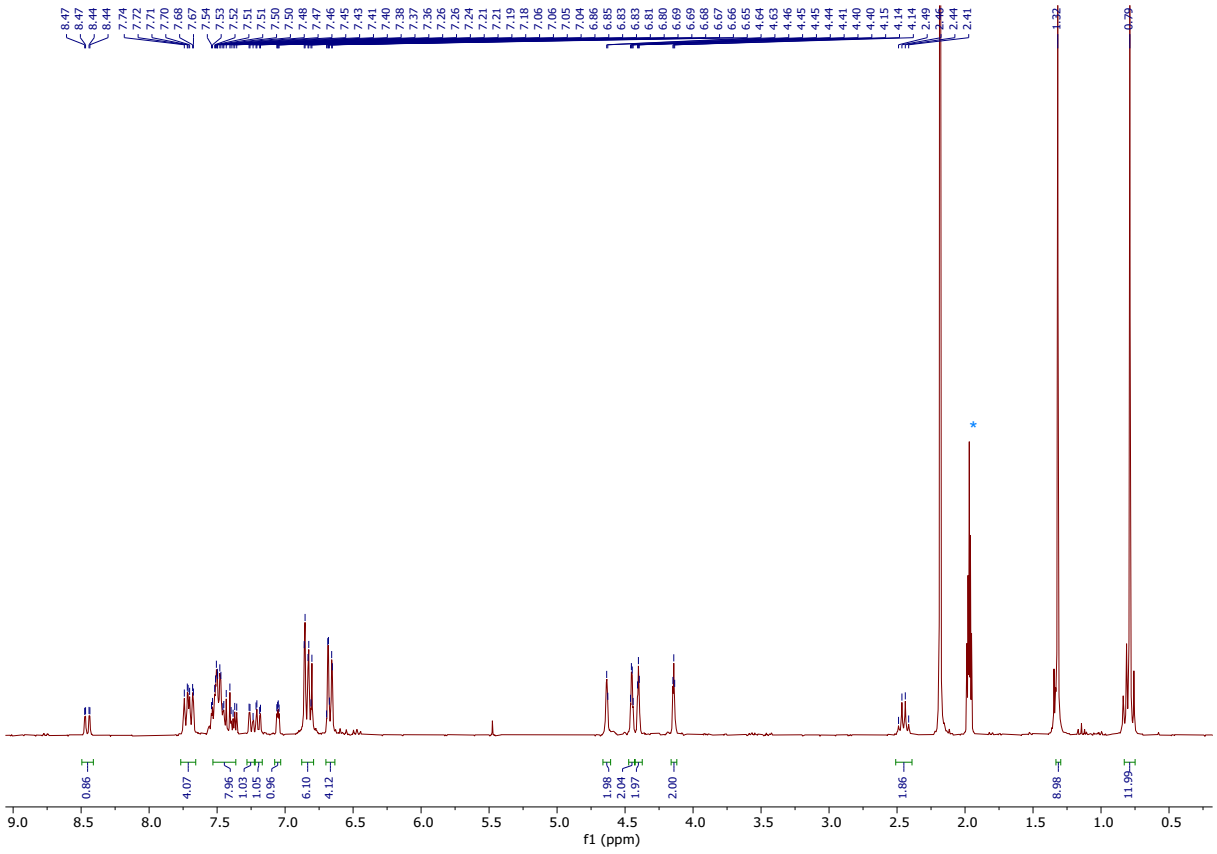

Figure S37. ^{1}H NMR spectrum (300 MHz, CD_3CN) of **8a**

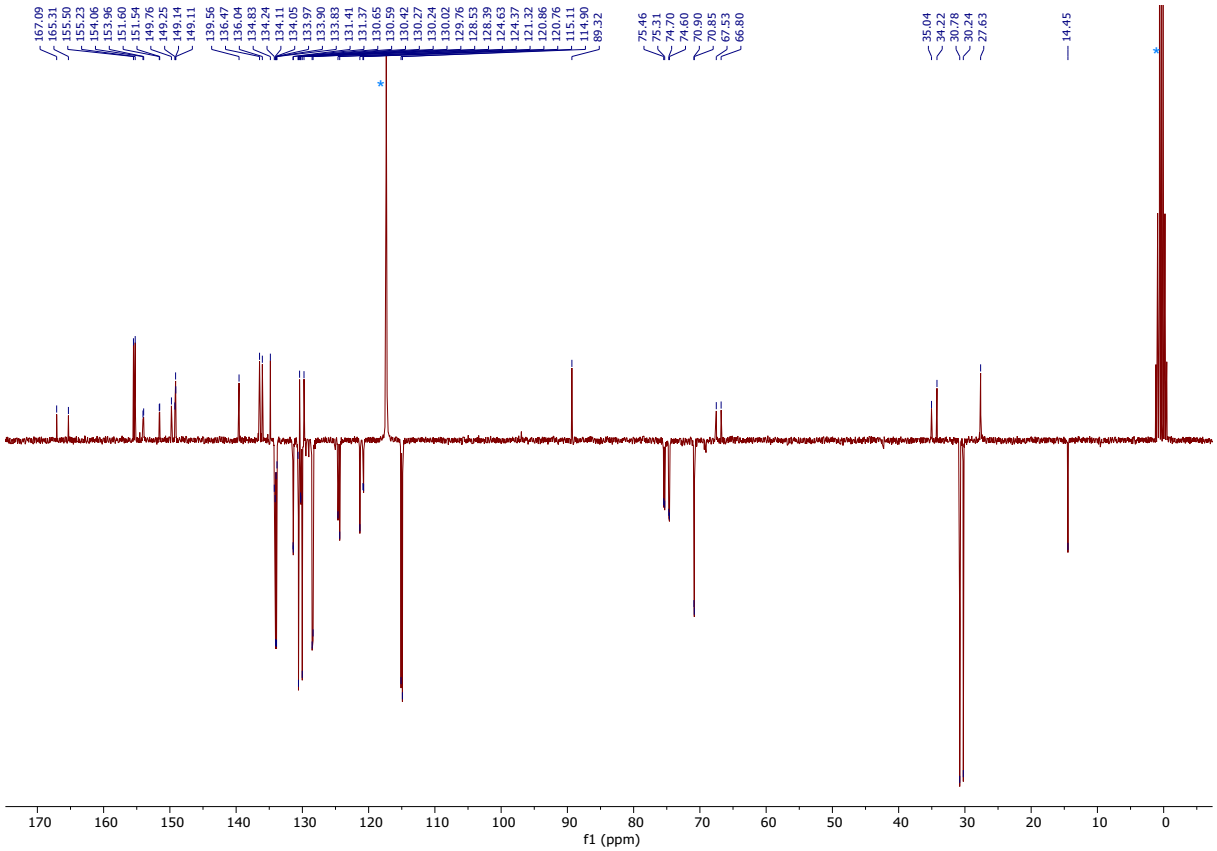

Figure S38. $^{13}C\{^{1}H\}$ NMR spectrum (75 MHz, CD_3CN) of **8a**

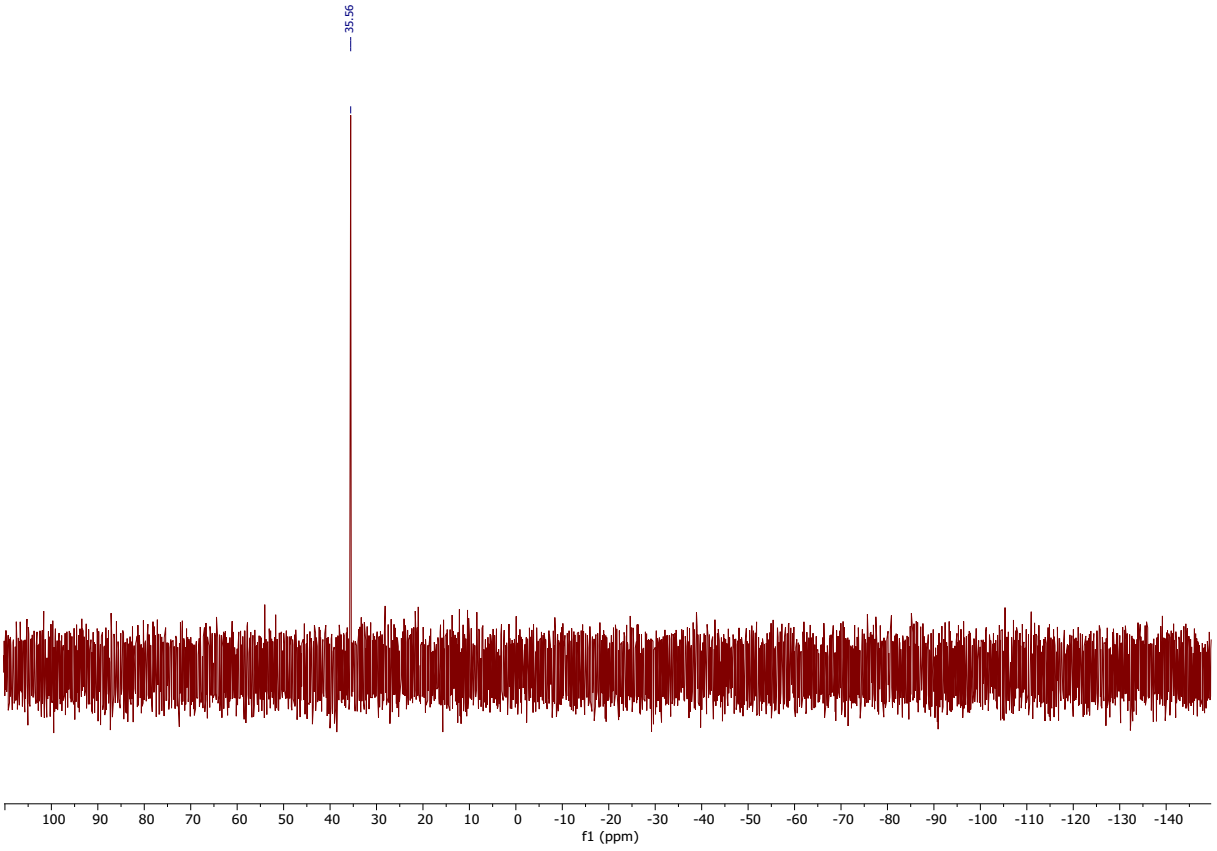

Figure S39. $^{31}P\{^{1}H\}$ NMR spectrum (122 MHz, CD_3CN) of **8a**

Table S4: Crystallographic data for **[(C^C)AuCl]$_2$** and **4b**.

	[(C^C)AuCl]$_2$	4b
CCDC deposition number	*2468916*	*2468917*
Empirical formula[a]	$C_{40}H_{48}Au_2Cl_2$	$C_{50}H_{57}AuCl_2F_6FeN_2P_2$
Moiety Formula	$C_{40}H_{48}Au_2Cl_2$	$[C_{49}H_{55}AuFeN_2P][PF_6]\cdot CH_2Cl_2$
Formula weight (g/mol)	993.61	1185.63
Temperature (K)	200	200
Crystal system	Monoclinic	Triclinic
Space group	$P2_1/c$	P-1
a (Å)	14.543(7)	13.1491(7)
b (Å)	5.976(3)	14.0080(7)
c (Å)	20.466(10)	14.7986(8)
α (°)	90	81.866(2)
β (°)	97.769(10)	73.881(2)
γ (°)	90	78.051(2)
Volume (Å^3)	1762.2(15)	2551.6(2)
Z	2	2
ρ_{calc} (g/cm^3)	1.873	1.543

[a] Including solvent molecules (if present).

[b] $R1 = \sum ||F_o| - |F_c|| \,/ \sum |F_o|$, [c] $wR2 = \sqrt{\sum \left(w\left(F_o^2 - F_c^2\right)\right) / \sum \left(w\left(F_o^2\right)^2\right)}$.

References

1 M. Křelinová, M. Salmain, P. Štěpnička, I. Císařová, B. Bertrand and J. Schulz, *ChemistryEurope*, 2025, 2500048.

2 V. Giuso, J. Yang, J. Forté, H. Dossmann, C. Daniel, C. Gourlaouen, M. Mauro and B. Bertrand, *ChemPlusChem*, 2023, **88**, e202300303.